ACCSCIENCE PUBLISHING

International Journal of Bioprinting

REVIEW ARTICLE

Vascular function in bioprinted skin and implications for wound repair

Lei Ru[1], Zhijian Liu[2], Xuwen Li[3], and Heng Wang[3]*

[1]Department of Bone and Joint Surgery, Fuyang Cancer Hospital, Fuyang, Anhui, China

[2]Department of Dermatology, The Third People's Hospital of Bengbu, Bengbu, Anhui, China

[3]Department of Plastic and Burn Surgery, The First Affiliated Hospital of Bengbu Medical University, Bengbu, Anhui, China

Abstract

Vascular markers, lumen-like structures, and fluid-conducting channels provide evidence of vascular cell identity, structural organization, and channel patency, respectively, in bioprinted skin. This critical narrative review examines how bioink design, cellular organization, and network architecture relate to measured transport and host-circulation access. A purposively assembled core of 19 primary or translational studies and 10 reviews informs the synthesis. We describe each vascular observation using independent fields for assay, compartment, endothelial source, observation time, model context, and construct relevance. Transient injection-assisted patency, sustained channel perfusion, and endothelial permeability are evaluated separately. Host angiogenesis, regional wound blood flow, and structural contact are distinguished from blood or circulating-tracer access localized to graft-associated vessels. Selected printed-skin studies demonstrate source-resolved host access in immunodeficient implantation models, whereas several transport principles come from skin chips or non-skin platforms. Four core studies treat newly excised wounds in diabetic animals; the clinical diabetic-foot-ulcer series has no vascular endpoint. These observations do not establish durable graft-specific vascular integration in clinical chronic ulcers. The review connects assay interpretation with bioink design and proposes product-specific reporting and validation priorities. Preserved search records and the core study registers are provided, while incomplete screening records, retrieval limits, and full-text availability constrain coverage. The synthesis is not a systematic review, meta-analysis, or estimate of evidence prevalence across the field. Clinical studies of chronic ulcers are needed to establish whether host blood reaches graft vessels and how long that access persists.

Keywords: Bioprinting; Vascularization; Chronic wounds; Bioink; Perfusion; Host integration; Skin tissue engineering

***Corresponding author:**
Heng Wang
(hengwang718@gmail.com)

Citation: Ru L, Liu Z, Li X, Wang H. Vascular function in bioprinted skin and implications for wound repair. *Int J Bioprint*. doi: 10.36922/IJB026390419

Received: September 22, 2026

Revised: October 29, 2026

Accepted: November 3, 2026

Published online: November 26, 2026

Copyright: © 2026 Author(s). This is an Open-Access article distributed under the terms of the Creative Commons Attribution License, permitting distribution, and reproduction in any medium, provided the original work is properly cited.

Publisher's Note: AccScience Publishing remains neutral with regard to jurisdictional claims in published maps and institutional affiliations.

1. Introduction

A bioprinted skin graft needs to go beyond merely restoring skin surface coverage. It requires adequate supply of oxygen and nutrients to its living dermis and a barrier to develop in the epidermis. This presents a mass-transport challenge: architectural resemblance alone cannot ensure adequate transport in thick or cell-dense constructs. In chronic wounds, impaired recipient-bed perfusion, inflammation, metabolic stress,

and infection can further delay vascular support after implantation. These restrictions are related to the state of the bed to which the skin is to be attached.[1-4]

Recent reviews organize skin bioprinting by bioinks, cells, fabrication routes, and regenerative applications.[5-13] Liu *et al*.[3] discuss bottom-up and top-down vascularization strategies, while Fang *et al*.[14] compare functional wound materials and printing technologies. A roadmap for perfused skin already distinguishes anatomical vascularization from transport, stability, and graft rescue, and an immune-focused review addresses immune-vascular incorporation.[15,16] The present contribution is an observation-level, non-ordinal synthesis: the same six descriptors are applied to identify what an assay establishes, where the result was measured, and how far it can be transferred to wound repair. The assay families and biological principles derive from prior work; their explicit separation and application to the selected study comparisons form the organizing proposal developed here.

The term *vascularization* can refer to very different observations. CD31 positivity supports endothelial-associated identity in an appropriate cellular and histological context but does not establish the presence of an open lumen. A lumen can be present without carrying flow. Dye passage can be used to assess channel patency but does not independently establish endothelial barrier function or sustained perfusion. Host vessels can increase regional blood flow without perfusing the printed construct. These differences matter when comparing chips, grafts, and bioactive dressings.[17-21]

Primary studies illustrate both advances in vascular function and the limitations of the available functional evidence. Host-injected lectin has reached human endothelial-lined vessels in printed skin grafts.[22,23] Other constructs have enhanced wound closure, collagen organization, or angiogenic histology without tracking flow through printed cells or channels.[17,24-27] Both of these endpoints are important and should be addressed independently from one another. Antioxidant, platelet-based, extracellular vesicle-based, or oxygen-generating formulations designed to treat disease may improve the recipient tissue environment but do not necessarily produce an intrinsically perfusable graft.[19,24,28-31]

This review examines vascular function in bioprinted skin and its implications for wound repair. Its primary focus is what individual assays establish about a defined printed or graft-associated compartment. We describe assay, compartment, endothelial source, observation time, model context, and construct relevance independently, without assigning a numerical vascular grade. Chronic wounds are a demanding potential application, rather than a setting in which the assembled evidence establishes functional graft integration. Non-printed skin, non-skin vascular platforms, and non-transplanted skin chips are discussed as contextual comparators for particular assays or design principles; their results are not attributed to implanted bioprinted skin.

2. Review approach and evidence framework

2.1. Review scope and literature records

This critical narrative review uses a purposively assembled reading library. The preserved discovery history has four distinct stages: seed discovery on August 14, 2026 (historical query rows HQ-01–21); targeted discovery on August 15 (HQ-22–41); contextual expansion on August 31 (HQ-42–52); and named-reference lookups on September 5 (HQ-53–59). Sources across these stages include Europe PMC, PubMed, Crossref, and OpenAlex, with publisher or repository retrieval and citation checks. Search concepts included skin, cutaneous, dermal, epidermal, wound, bioink, bioprinting, vascularization, perfusion, anastomosis, diabetes, ischemia, and infection. Supplementary Table 3 preserves the exact requests, dates, count semantics, and retrieval limits; the stage map in Supplementary Methods Notes explains the different selection purposes. Automated source and consistency checks extend through September 9. The stages were not successive filters applied to one common candidate universe.

The core analytic set contains 19 primary or translational studies with structured extraction and 10 reviews. Supplementary Table 1 lists each core primary record by stable Source ID, title, DOI, model, and actual vascular observation. Supplementary Table 2 lists the 10 core reviews separately; they are interpretive sources, not independent experiments. Supplementary Table 3 provides 59 preserved historical query records, including exact string, source, date, count semantics, retrieved records, and retrieval limits. Current reference numbers are mapped to the unchanged historical registers in Supplementary Table 4. Contextual references and targeted addenda have not all undergone the same full-field extraction and are excluded from the 19-study denominator.

The core is used as a set of assay and model contrasts, rather than a statistically representative sample of bioprinting research. Its analytic role is to compare observations in defined skin constructs, distinguish structural or repair outcomes from construct-localized flow, and examine limits on transfer to wound treatment. Marker-only studies and the clinical ulcer series without a vascular endpoint make these boundaries explicit. Non-

transplanted skin models and the non-skin flap study contribute only to the transport or connection questions they examine. This coverage fits the claim-interpretation objective, but does not establish that every relevant technology or study was captured. The 19-study count describes the registered reading set and is not a field-wide denominator.

The archived seed-stage rules prioritized English peer-reviewed work on skin or wound constructs, cell-laden bioinks, vascular assays, or translation, generally emphasizing 2021–2026 while retaining selected earlier methodological papers. Ordinary printed scaffolds without relevant living-cell content and duplicate or low-priority overlapping reviews were deprioritized at that stage. Targeted discovery subsequently sought contrasts in direct transport, host connection, disease background, and translation; contextual expansion and named-reference lookup supplied specific mechanistic or assay comparators. The final synthesis retained marker-only studies and a clinical series without a vascular assay because they expose limits of vascular interpretation. These stage-specific rules were not a single prospectively fixed eligibility protocol. Bioprinted-skin experiments supply direct construct evidence; non-printed skin, non-skin, and device-supported models contribute only to the questions they actually test.

The authors performed literature searches, initial selection, scientific data extraction, and preparation of the original scientific table content. Candidate discovery, deduplication, prioritization, and preliminary extraction are traceable in archived files. The seed archive records 415 retrieved records, 341 unique candidates, and 35 selected seeds. A read-only identity-set reconstruction finds 23 selected seeds within that candidate pool and 12 outside it; the 318 excluded or deferred identities equal 341 minus those 23 pool members. The 35 seeds and 318 records therefore have different denominators. This reconstructs set membership, not a complete human exclusion history. The August 15 archive separately records 1,113 retrieved and 812 deduplicated candidates with automated priority labels. Later searches include open-access filters and retrieval caps, including 20 PubMed IDs per query. No registered protocol, exhaustive search, documented independent dual-reviewer process, formal risk-of-bias assessment, or meta-analysis is established. The search archive supports repetition of recorded requests and identity checks, but not reconstruction of a complete prospective screening flow.

The contextual literature updates were conducted separately from the construction of the core evidence set. Three additional articles were included as contextual sources on October 12, 2026. Five further publications were individually assessed on October 29, 2026, through verification of their DOIs against publisher records and examination of their abstracts and available full texts. Of these, two addressed bioprinting or related material synthesis, whereas three provided comparisons involving non-printed wound materials. These updates do not involve a new systematic database search or alter the core evidence set comprising 19 primary or translational studies and 10 reviews. Details of the source-access scope for these additional publications are provided in the Supplementary Methods Notes.

OpenAI Codex assisted manuscript editing, source and citation consistency checks, formatting, and technical preparation of the supplementary material. In this revision, it also assisted in the comparison of published assay descriptions and checks of the five suggested contextual sources. The original author-verification scope is described in Section 2.3. Figure 1 was hand-drawn by the authors and edited using Adobe Photoshop. On October 15, 2026, the authors used an OpenAI image tool through Codex to help prepare the graphical abstract. The OpenAI image-tool interface did not display a version identifier. These schematics contain no experimental measurements.

2.2. Independent fields for interpreting vascular observations

Figure 1 sets out six parallel fields for describing each vascular observation: assay, measured compartment, endothelial source, observation time, model context, and construct relevance. Assay descriptions distinguish molecular or histological observations, injection-assisted lumen patency, sustained flow through a defined path, and endothelial permeability. Compartment identifies whether the observation concerns an independent cell-culture assay, a printed channel, a graft-associated lumen, or the whole wound. Source records donor, host, or mixed endothelium only when supported by an appropriate label. Observation time separates culture or implantation age from the actual period of observed flow. Model context reports species, immune status, disease background, and pre-treatment wound history. Construct relevance identifies bioprinted skin, a non-transplanted skin model, or a contextual non-skin/non-printed comparator. These fields are not summed, ranked, or treated as compulsory steps. An unperformed assay is unassessed, not evidence that vessels or flow are absent.

Transient injection, sustained pumping, and permeability testing answer separate questions. Tracer passage during a brief injection tests lumen patency under that condition. Pump-supported transport is described with fluid, flow rate or pressure, inlet/outlet definition, and measured duration. Endothelial permeability requires

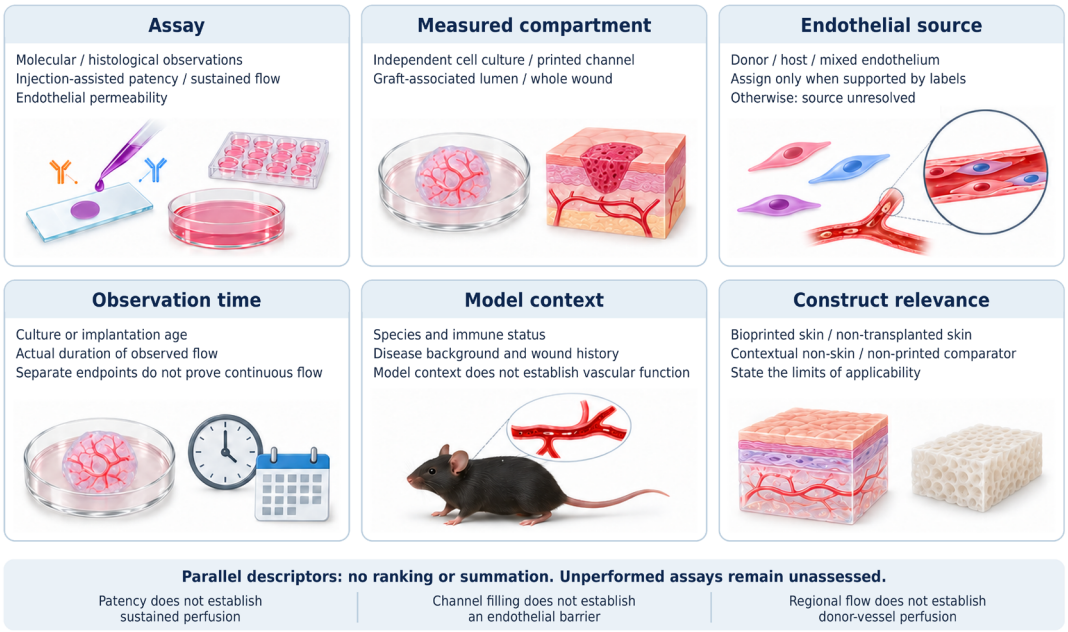

Figure 1. Six independent fields for interpreting vascular observations. The six panels record assay, compartment, endothelial source, observation time, model context, and construct relevance in parallel. A study can report several assays, each with its own compartment and temporal limits. Injection-assisted patency does not establish sustained perfusion; flow through a non-endothelialized channel does not establish an endothelial barrier. Regional wound flow and host angiogenesis do not identify donor-vessel perfusion. Species and immune status describe the model and do not substitute for measured vascular function. No numerical grade, validated clinical hierarchy, or compulsory assay sequence is proposed. This conceptual schematic contains no experimental measurements. Figure 1 was hand-drawn by the authors and edited using Adobe Photoshop.

an identified endothelial wall, tracer properties, and appropriate non-endothelialized controls; it is not inferred from channel filling alone. *In vivo*, intraluminal host erythrocytes, a terminal circulating tracer, and repeated live-flow imaging provide different temporal information. Host-circulation access must be localized to graft-associated vessels, with endothelial source stated where resolved. Repeated terminal observations at different implantation ages do not establish uninterrupted flow between those time points. Species, immune status, and wound history remain separate applicability fields.

The six-field arrangement is an organizing proposal for this review. It adapts established distinctions among fabrication, transport, host connection, and model suitability into one observation-level record. Earlier reviews already address material functions, multiscale vascular strategies, perfusion benchmarks, and immune-vascular interactions.[3,14-16,32] The additional step here is to keep these descriptors independent when comparing specific study claims, rather than to introduce new vascular biology or a validated grading instrument.

2.3. Data extraction and source verification

Structured data extraction included formulation, fabrication methods, cell types, construct dimensions, experimental models, sample characteristics, controls, vascularization assays, observation periods, and source references. Heng Wang conducted the literature searches and screened the records. Codex assisted with preliminary data extraction and organization. Heng Wang verified the extracted data against the source publications for all 19 core primary or translational studies. Zhijian Liu reviewed selected original publications and checked key vascular findings.

Assays that were not performed were classified as "not assessed," whereas information absent from the source examined was classified as "not reported" (NR). Unavailable sources, unverified entries, and unresolved discrepancies between sources were documented separately. Independent duplicate screening and formal disagreement adjudication are not documented. No formal risk-of-bias assessment is reported.

Wound history was evaluated independently of vascularization measurements. Wound models were distinguished as healthy acute excisions, acute wounds induced in diabetic or ischemic animals, established experimental nonhealing wounds, or clinically diagnosed ulcers. Preintervention wound chronicity was determined based on documented wound history rather than

underlying disease status alone. Experimental wounds were classified as nonhealing only when a period of impaired healing before intervention was documented. Clinical ulcer diagnoses and baseline wound durations were recorded when reported. High-glucose, hypoxic, oxidative, and inflammatory cell culture assays were categorized as mechanistic models rather than direct evaluation of chronic-ulcer treatment efficacy. Changes in regional blood flow were distinguished from construct-specific vascular function, which required direct supporting evidence. Vessel dimensions were extracted from explicitly reported source measurements and were not estimated from scale bars.

3. Why chronic wounds change the vascularization problem

3.1. Chronic wounds create a hostile environment for vascularization

A chronic wound is not merely an acute wound that lasts longer. In patients with diabetes, macrovascular disease, microangiopathy, neuropathy, immune dysfunction, altered fibroblast and keratinocyte activity, and impaired extracellular matrix turnover may coexist. Local hypoxia exists with impaired hypoxia-responsive repair; resident and delivered cells are damaged by oxidative stress; chronic inflammatory signaling exists with proteases that destabilize the matrix; bacterial burden and biofilm consume resources and prolong inflammation. In diabetic foot ulcers and chronic-wound bioinks, reviews point out that a construct should not only target cells, but also the underlying defects of these highly interacting conditions.[1,2,4,33]

Mechanistic wound models can isolate selected components of this hostile environment, but disease-associated experimental conditions must be interpreted in their anatomical and experimental contexts. Tan *et al.*[34] reported that high-glucose conditions impair keratinocyte, fibroblast, macrophage, and endothelial cell (EC) functions, highlighting the need to evaluate multiple cell populations rather than ECs alone. A complementary non-printed skin equivalent was constructed using a leukocyte-depleted platelet-rich plasma (PRP) matrix containing fibroblasts and epithelial cells, followed by scratch injury and exposure to recombinant tumor necrosis factor. The measured outcomes included gene expression and protein secretion of interleukin-8 and transforming growth factor-α.[35] This is evidence that can be used for inflammatory perturbation in an organotypic skin equivalent. Although the authors related their model to poorly perfused wounds, it did not incorporate a vascular circuit or directly reproduce reduced blood flow. Such inflammatory perturbation models can complement cell-response assays before vascular function is evaluated in perfused constructs.

Mechanistic studies support distinguishing oxygen availability from cellular responses to oxygen deprivation. In db/db mice, Botusan *et al.*[36] found reduced wound hypoxia-inducible factor 1 alpha (HIF-1α) despite greater hypoxia; hydroxylase inhibition or stabilized HIF-1α gene transfer enhanced healing and histological vascular measures. In complementary human-specimen and mouse studies, diabetic wound-conditioned medium maintained inflammatory macrophage signaling. Local interleukin-1 beta or inflammasome inhibition enhanced re-epithelialization and granulation in diabetic mice without increasing CD31 staining in the corresponding pharmacological experiments.[37,38] These native-wound and independent cell-culture findings offer mechanistic context for bioink design. They also show why improved repair alone does not establish that an implanted construct has acquired a perfused vascular network.

The repair studies are aimed at the disease and exhibit several design responses. A curcumin-containing gelatin methacryloyl (GelMA) construct protected adipose-derived stem cells (ADSCs) from advanced-glycation-end-product-associated oxidative injury and improved their survival in diabetic wounds, but vascular evidence was limited to wound-tissue CD31 and α-smooth muscle actin (α-SMA) staining; the construct contained no ECs and no lumen or tracer-based flow was shown.[19] A collagen-based bioink for digital light processing (DLP) was optimized for diabetic wound repair and produced vessel-like profiles and vascular morphometry, yet did not directly demonstrate flow or host–graft inosculation.[39] An all-peptide click-chemistry platform printed vascular-related cells and promoted diabetic wound healing, with vessel-like structures and vascular markers but no construct-specific perfusion test.[40] These studies contribute to cell protection, matrix design, and reparative signaling; they do not directly demonstrate flow through a printed vascular compartment.

This is particularly clear in oxygen-directed strategies. Photosynthetic scaffolds can produce oxygen and facilitate wound healing, and microalgae gels with a programmed function and oxygen-sensitive grafts show potential for a responsive chronic-wound system.[28,30,41] Increased oxygen production does not guarantee cell survival and may facilitate angiogenesis, but oxygenation does not demonstrate vascular perfusion and cannot be used in isolation to imply that the repair effect was due to the development of new vessels. For microbial systems that are living, the duration of oxygen availability must also be considered in relation to immune recognition,

environment, antimicrobial co-therapies, containment, and the possibility that illumination requirements may differ across anatomical sites.

Another layer of design is added with infection. Though photoactive composites are used for both antimicrobial and repair functions,[42] and herbal/microalgal scaffolds have been used for oxygenation and modulation,[43] the antimicrobial, cytocompatibility, barrier, and perfusion properties must be determined separately; a bactericidal dose may harm endothelial cells, while a sprouting-optimized matrix may be sensitive to proteases or biofilm-associated degradation. Chronic-wound bioprinting therefore requires factorial designs to evaluate vascular constructs under the same high-glucose, hypoxic, inflammatory, and microbial conditions as seen in the indication.

Cellular stress is time-sensitive. In acute, nondiabetic mouse wounds, Demaria *et al.*[44] reported transient senescent fibroblast and endothelial populations; the reported removal of these cells delayed wound closure, whereas treatment with platelet-derived growth factor AA restored wound closure kinetics and myofibroblast differentiation. However, a formal Expression of Concern was published for this study in 2026, warranting cautious interpretation of its findings. These findings do not establish the effects of persistent senescence in diabetic ulcers or the efficacy of senescence-targeted grafts. Stress-associated markers should therefore be interpreted in relation to cell identity, timing, and wound context.

3.2. The recipient bed can confound vascular readouts

Laser speckle contrast analysis, Doppler-based methods, and appropriately validated photoacoustic flow measurements can provide information about regional perfusion, but without spatial or lineage resolution, they cannot distinguish blood flow around the implant from flow through host vessels or the printed network. In diabetic wounds, increased laser-speckle flow accompanied healing, but the signal was not traced to the printed endothelial structures; this supported repair-associated regional perfusion without establishing host blood access to the printed vascular compartment.[40] Likewise, increased $CD31^+$ area may reflect host angiogenesis and does not itself demonstrate flow through a graft.

Construct-specific functional evidence requires direct flow or tracer observations localized to the construct, for example, circulating tracer combined with human-specific and host-specific endothelial labeling, known inlet/outlet perfusion, or imaging of flow across anastomotic junctions. Printed-cell tracking can establish source attribution but does not by itself establish perfusion. Without such attribution, wound-level flow is a complementary outcome and does not establish construct perfusion. This is most important for chronic models, since the capacity to enhance host angiogenesis may be useful even if printed material is used primarily as a signaling depot.

4. Bioink design as a vascular microenvironment

The material comparison begins with direct experiments on printed skin or wound constructs. Table 1 aligns fabrication and bioink choices with four separate outcomes: endothelial-cell survival evidence, lumen formation, perfusion, and host access. Studies without printed ECs remain informative for wound repair but cannot establish survival or flow of a delivered endothelial network. Contextual material and non-skin examples are used only where they clarify a particular design or assay question.

4.1. Printability, transport, and remodeling are coupled

Bioink choice must support reproducible deposition and the cells that remodel or line the construct. Figure 2 summarizes conceptual design requirements. Table 1 compares their experimental support rather than inferring function from formulation or printer type; the original detailed manufacturing examples are retained in Supplementary Table 4. No matched head-to-head comparison supports a ranking of printing technologies.[18,19,23,24,40]

Bioink design is typically considered in terms of a balance of print fidelity and cell viability. In the case of vascularized skin, the trade-off is much wider: the viscosity, yield stress, crosslink density, fiber architecture, swelling, degradation, ligand presentation, and porosity all need to be considered in determining whether ECs can survive printing, form lumens, remodel the matrix, and exchange solutes under flow. A formulation can print a sharp lattice yet restrict cells within a dense network; a permissive collagen or fibrin gel can support morphogenesis yet may contract, deform, or lack mechanical durability. This materials–biology trade-off has been reviewed in reviews of skin bioinks.[2,5,6,13,33]

The direct GelMA examples illustrate why material names do not predict vascular function. Hybrid coaxial/extrusion printing produced channels with injection-assisted passage, whereas curcumin–GelMA delivered ADSCs without printed ECs, and GelMA/methacrylated silk fibroin delivered fibroblasts.[18,19,25] Tissue-derived additives, bioglass, and adipose spheroids broaden the design space, but do not supply a shared vascular endpoint.[45-48] Polymer concentration, modification,

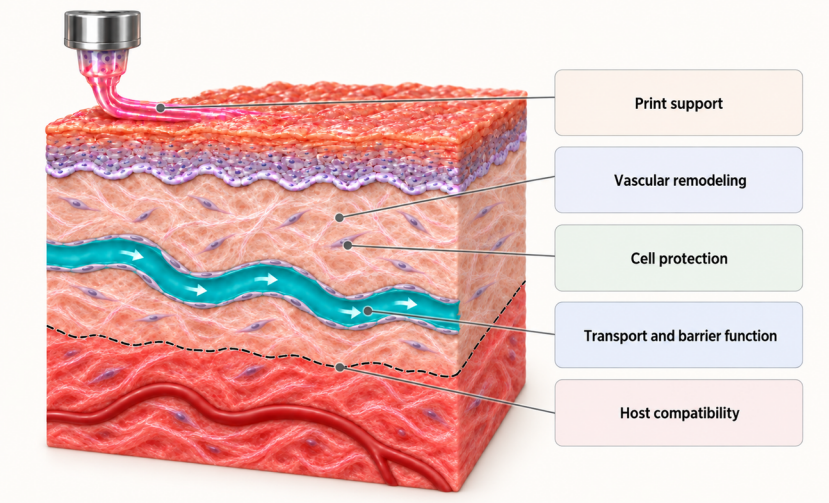

Figure 2. Bioink design requirements for vascularized skin. The idealized skin cross-section illustrates an epidermal layer, a cell-bearing dermal matrix, a blue-green designed vascular channel, and underlying red host vasculature. The black dashed line denotes the proposed graft–host interface. White arrows within the designed channel indicate proposed transport direction, not measured or sustained perfusion or established endothelial barrier function. The printing nozzle and tissue structure jointly summarize fabrication and design concepts; they do not depict a validated procedure for generating dermal vessels by printing onto an intact epidermis. The five labels identify design requirements rather than experimental readouts. Host angiogenesis does not establish graft-vessel perfusion. The diagram is a conceptual synthesis, not a fabricated construct, measured anatomical section, or demonstrated combination of interventions. Dimensions and connections are illustrative, not to scale. Figure created by the authors with Adobe Photoshop based on the reviewed design considerations.[18,19,23,24,40]

initiator, light exposure, and secondary crosslinks must therefore be reported with the particular cell and flow assay.

Reviews of GelMA and extrusion printing describe the general balance between gel mechanics, remodeling, and print fidelity.[49,50] In a contextual microcarrier/hyaluronic acid (HA) system, implanted human fibroblasts and dermal matrix persisted during a 28-day experiment; separate vascular stains did not establish CD31/α-SMA colocalization or a perfused endothelial network.[51] This supports cell-delivery design rather than a direct vascular-function comparison.

The bioinks with high collagen content better simulate the dermal matrix and aid endothelial morphogenesis, but their slow gelation and poor mechanics point to hybrid approaches. Layered *in situ* printing used a gelatin/alginate bioink with PRP; fibrinogen/fibrin belonged to the PRP component rather than a separately specified base polymer. Tubule-like CD31-positive structures and enhanced healing were observed, but direct flow was not evaluated.[24] Active medium circulation around high-concentration collagen constructs enhanced viability and metabolic activity, demonstrating that material choice was related to culture operation; it did not establish intraluminal transport through an endothelial network.[52] High-resolution collagen printing provides internally perfusable, fully biological architectures, but translation to skin requires endothelialization, barrier testing, and compatibility with epidermal maturation.[53]

Tissue-derived and recombinant matrices provide contextual alternatives: skin extracellular matrix/fibrinogen improved material and cell-support properties, and gelatin/recombinant collagen supported printing and wound repair.[54,55] In a separate recombinant-collagen/GelMA study, the rat treatment was a precursor hydrogel, not transplantation of the complete printed dermo-epidermal equivalent.[56] These endpoints should not be pooled as evidence of graft perfusion.

Peptide, HA, silk, nitric-oxide, and placental formulations offer matrix or payload options.[25,31,40,42,57-59] Their vascular interpretation depends on the delivered cells and the tested compartment: host angiogenic responses to a dressing do not establish a preformed perfused graft network.

4.2. Endothelial cells require positional and cellular support

The inclusion of ECs in a construct is necessary for many prevascularization strategies but is not sufficient to establish stable vasculature. Lumen formation and host interaction are influenced by source, passage, density, distribution, and phenotype. Primary dermal microvascular ECs are relevant and difficult to expand; human umbilical vein endothelial cells (HUVECs) are accessible but not skin-specific;

Table 1. Printing routes and bioinks compared by endothelial survival, lumen, perfusion, and host access

Study and printing route	Bioink and cells	EC viability evidence and lumen formation	Perfusion observation	Host access and model boundary
ITOP pneumatic extrusion[17]	Fibrinogen/gelatin/HA; six-cell layered skin including HDMECs	EC-specific fraction NQ; post-implant ZO-1-positive lumens without EC-specific fate tracing	No direct flow or circulating-tracer assay in the checked study	Acute nude-mouse wounds; repair and vascular morphology do not establish graft-vessel flow
Robot-assisted *in situ* extrusion[24]	Gelatin/alginate/PRP; fibroblasts and epidermal stem cells, no printed ECs	Non-EC viability cannot establish EC survival; wound CD31-positive tubule-like profiles	Direct lumen flow/tracer access unassessed	Fresh rat wounds; angiogenic histology and repair, without source-resolved graft vessels
Hybrid coaxial and extrusion[18]	SA/GelMA vessel walls and GelMA layers; printed HUVEC compartments plus luminal EC seeding	EC-specific fraction NQ; hollow channels and confluent HUVEC coverage	Injection-assisted dye patency (10 s); 40-kDa dextran transport; mature endothelial barrier unverified	Unimplanted skin construct; no host integration experiment
Extrusion[25]	GelMA/SilMA; mouse dermal fibroblasts, no printed ECs	Fibroblast viability is not EC survival; continuous endothelial lumen unassessed	Direct construct flow/tracer access unassessed	Acute mouse wounds; reparative and vascular-histology outcomes
DLP[40]	Thiol-ene all-peptide gamma-PGA hydrogel; VEGF165-overexpressing HUVECs	Post-print GFP/CCK-8 and proliferation; no EC-specific viable fraction or continuous printed lumen established	LASCA wound-region flux; not printed-vessel flow	Fresh STZ-rat wounds; vascular source unresolved
Extrusion[19]	GelMA/curcumin; human ADSCs, no printed ECs	ADSC protection/survival cannot substitute for EC viability; CD31/α-SMA in wound tissue	No lumen or direct flow assay	Fresh STZ-nude-mouse wounds; host repair rather than a traced perfused graft network
DLP[39]	Collagen methacrylate/DHM; HDF wound construct, HUVECs in separate printability tests	HDF Live/Dead and HUVEC printability remain separate; no perfused endothelial lumen in the treatment construct	Wound vessel morphometry; no direct construct perfusion test	Fresh diabetic-rat wounds; HUVEC test models were not the implanted treatment
Extrusion with self-assembly[23]	Xeno-free collagen-I/fibronectin/VitroGel/PGA mesh; ECs, pericytes, fibroblasts, and keratinocytes	EC-specific post-print fraction NQ; human EC-lined vessels after implantation	Host-infused Ulex accesses human vessels at separate 2-, 4-, and 6-week endpoints	Acute immunodeficient graft model; terminal access is not continuous six-week flow
Extrusion with self-assembly[22]	Collagen-I dermis; ECs, fibroblasts, pericytes, and keratinocytes	Calcein-positive networks and open lumens; EC-specific viable fraction NQ	No *in vitro* pump assay; tail-vein UEA-I labels human vessels at four weeks	Acute severe combined immunodeficiency/beige graft model; terminal source-resolved host access
Extrusion with sacrificial channels and EC seeding[21]	GelMA dermis/epidermis, sacrificial Pluronic; printed BJ/HUVEC co-culture and post-seeded channel	Mixed dermal-cell viability, not an isolated EC fraction; endothelialized main lumen	Pumped dextran transport; 70-kDa permeability tested against non-endothelialized channels	Unimplanted skin-on-chip; device-supported flow is not host integration

Note: This table presents selected study-level comparisons rather than direct comparisons of printing technologies or a pooled performance analysis. NQ indicates that an EC-specific post-print viable fraction was not available for comparison; it does not imply cell death or the absence of viability testing. Mixed-cell viability, preprinting assessments, and viability measurements involving other cell types are distinguished in the corresponding entries. The absence of direct flow testing indicates that construct-specific perfusion was not assessed, rather than demonstrating an absence of perfusion. Detailed formulations and operating conditions are provided in Supplementary Table 4 and the core study registers. Additional information on assessment ages, operating conditions, and observation intervals is provided in Table 2.

Abbreviations: ADSC: Adipose-derived stem cell; BJ: Human neonatal foreskin fibroblast cell line; CCK-8: Cell Counting Kit-8; CD31: Cluster of differentiation 31; DHM: Dihydromyricetin; DLP: Digital light processing; EC: Endothelial cell; GelMA: Gelatin methacryloyl; GFP: Green fluorescent protein; HA: Hyaluronic acid; HDF: Human dermal fibroblast; HDMEC: Human dermal microvascular endothelial cell; HUVEC: Human umbilical vein endothelial cell; ITOP: Integrated tissue–organ printer; LASCA: Laser speckle contrast analysis; NQ: Not quantified; PGA: Poly(glycolic acid) (mesh); PRP: Platelet-rich plasma; SA: Sodium alginate; SilMA: Methacrylated silk fibroin; STZ: Streptozotocin; UEA-I: *Ulex europaeus* agglutinin I; VEGF165: Vascular endothelial growth factor A isoform 165; ZO-1: Zonula occludens-1; α-SMA: α-smooth muscle actin; γ-PGA: poly(γ-glutamic acid).

endothelial colony-forming cells and induced pluripotent stem cell (iPSC)-derived ECs offer scalable or personalized alternatives, with additional questions about maturity, genomic stability, and lot consistency.[12,60]

Controlled microvascular models show that support-cell effects are context-dependent. In molded collagen microchannels lined with HUVECs, Zheng *et al.*[61] observed endothelial sprouting or retraction after adding brain-derived pericytes, with permeability differing between these outcomes and culture conditions. Their blood-perfusion tests distinguished relatively nonadhesive quiescent vessels from phorbol 12-myristate 13-acetate-stimulated vessels with platelet accumulation. These were molded, in vitro networks rather than printed skin grafts. They provide a methodological example of jointly measuring mural-cell association, barrier properties, and blood–endothelium interactions, while retaining cell-source and culture-condition differences when interpreting results.

Supporting cells (pericytes, fibroblasts, ADSCs, spheroids) supply basement-membrane components, angiogenic signals, and mechanical support.[12] A four-cell vascularized skin graft (keratinocytes, fibroblasts, pericytes, ECs) showed that human endothelial-lined vessels were reached by host tracer.[22] A xeno-free graft combined ECs, placental pericytes, fibroblasts, and keratinocytes; tail-vein lectin reached human endothelial-lined graft vessels post-implantation.[23] Spatially controlled constructs with primary or iPSC-derived ECs combined perfusable patterned channels *in vitro* with systemically perfused host vessels in the graft region *in vivo*, but did not directly show host blood traversing the human channel or image a human–mouse junction.[60] In contrast, a coaxial skin-organoid model produced luminal structures and endothelial junction markers but lacked a post-print perfusion assay, illustrating why morphology does not establish flow.[62]

Secretome assays measure responses to signals released by cellular constructs outside of the graft. Printed sacrificial molds were used to cast collagen sheets containing ECs and ADSCs. Their supernatant was used to treat HUVECs on Matrigel, with no statistically significant difference in the reported tube metrics.[63] Patient-derived matrix models also tested conditioned medium on a separate basement-membrane substrate.[64] In the photosynthetic scaffold study, HUVECs were seeded on Matrigel in a 24-well plate, and scaffold-bearing Transwell inserts were placed above them for a six-hour tube-formation assay.[28] This independent assay measures tube formation outside the printed construct; neither the printed hollow geometry nor wound CD31 staining shows a perfused endothelial channel. Such tests measure responses to the surrounding treatment environment, while graft-function tests interrogate the constructed vascular compartment.

Support-cell ratios cannot be optimized independently of matrix, culture time, and intended vessel compartment. Spheroid, organoid, and endothelial-coated-microsphere approaches provide contextual routes for organizing cells or recruiting host vessels, but source tracing is required to distinguish donor-vessel formation from host recruitment.[46,65-67]

Adipose preparations also have different identities. Microfat printing preserved tissue activity without testing vascular function, whereas a collagen-microfiber/fibrin construct containing adipocytes, stromal cells, and HUVECs showed luminal architecture and adipocyte function.[68,69] These observations cannot be treated as equivalent endothelial-survival or flow measurements.

When it comes to translation, the identity of the vascular cells should be regarded as a key material characteristic. Minimum cellular characterization should include, as appropriate, endothelial junction and basement membrane markers, mural-cell coverage, inflammatory activation markers, cell source, donor number, passage number, cell density, viability immediately after printing and during maturation. For pluripotent stem cell-derived populations, assessment of residual undifferentiated cells should also be considered. These properties assist the assessment of the repeatability of functional outcome.

4.3. Bioactive modules should be linked to a vascular mechanism

The use of antioxidants, platelet products, exosomes, oxygen generators, nitric oxide, or antimicrobial agents has attracted considerable attention in chronic-wound bioinks. Bioactive formulations should link their payload-release characteristics to a prespecified vascular mechanism of action. For instance, curcumin can be evaluated through reactive oxygen species, apoptosis, and implanted-cell survival readouts before interpreting vascular-histology claims; PRP should be evaluated by composition and release kinetics, not as a generic growth factor mixture; engineered M2-macrophage exosomes should be assessed with inflammatory polarization and angiogenic signaling assays.[19,24,29] Thermoresponsive antioxidant bioinks and biomineralizing hydrogels should also be tested for dose–response, release, and endothelial safety assays, targeting diabetic-wound stress.[70,71]

Payload and cell-delivery experiments clarify recipient-bed effects. ADSC- or conditioned-medium-loaded GelMA/alginate methacrylate, extracellular-vesicle-retaining umbilical-cord matrix, and vesicle-loaded conductive hydrogels evaluated inflammatory, oxidative,

or repair-associated endpoints.[72-74] Independent endothelial assays and wound histology address different compartments; neither supplies a missing graft-flow test.

Regional perfusion, blood-vessel markers, and lymphatic markers also require separate attribution. Zinc/silicon–GelMA, a non-printed cyanobacterial scaffold, and a printed polysaccharide/chitosan/gelatin dressing illustrate these distinct payload-related readouts.[75-77] They inform host repair and stress modulation rather than a pooled measure of printed-vessel performance.

Mechanistic studies should also be carried out to test for necessity. If oxygenation is claimed to drive vascularization, an oxygen-matched control and an angiogenesis-inhibited condition can help distinguish direct causation from parallel effects. When a specific extracellular vesicle cargo is proposed to stabilize vessels, cargo depletion or blockade of the implicated pathway can help establish mechanistic specificity. If these are not included, the outcome should be presented as an association of the bioactive module, repair, and vascular readouts. This is not just semantic prudence; mechanism-based release specifications should be considered when an intricate bioink advances toward production under good manufacturing practice conditions.

Zhang *et al.*[78] combined an extracellular-vesicle-loaded, decellularized skin matrix with a Cu_2O–polycaprolactone layer, demonstrating *in vitro* methicillin-resistant *Staphylococcus aureus* inhibition and improved repair with increased wound CD31 staining in newly created full-thickness defects in db/db mice. These endpoints support antibacterial delivery and host repair, while the reported vascular assays do not establish flow through a printed graft network.

Cao *et al.*[79] spatially separated silver-containing chitosan from silk-methacrylate hydrogel carrying epidermal-stem-cell exosomes and metformin. The wound experiment topically applied hydrogel formulations 24 hours after bacterial inoculation of newly excised diabetic-mouse wounds; improved closure and CD31 staining therefore support repair by a compartmentalized dressing, without establishing transplantation or perfusion of a complete printed skin graft.

5. Engineering perfusable networks

For a designed-channel construct intended for perfusion before implantation, lumen passage, sustained flow, and endothelial barrier testing answer separate questions. A self-assembling graft requires a different schedule because host flow may arise after implantation, as discussed in Section 8.2.

5.1. From endothelial identity to an open lumen

Molecular and structural observations are biologically meaningful. Endothelial and mural markers help characterize cells, but markers such as zonula occludens-1 (ZO-1) and α-SMA are not vascular-lineage specific; context and co-labeling are important.[17,19] Three-dimensional rings, tubes, and central spaces suggest lumen-like morphogenesis, but these observations alone cannot establish a continuous inlet–outlet path, lumen patency, or leak resistance.

Skin studies show diverse anatomical findings. Full-thickness printed skin showed ZO-1-positive lumens postimplantation, but lacked endothelial fate tracing or circulating-tracer tests.[17] Other studies reported vessel profiles, tubule-like structures, or endothelial rings in wounds.[24,27,39] The robotic human skin substitute demonstrated human–rat vascular connections and rat erythrocytes within human endothelial-lined lumens (Supplementary Figure S2 of Pontiggia *et al.*[80]), providing histological evidence that host blood reached graft vessels at the sampled time point. However, the duration of flow was not measured.

5.2. Fabrication strategies for direct flow

Several approaches can establish a flow path. Sacrificial printing deposits a removable filament within a bulk matrix, leaving a channel that can be endothelialized. Coaxial printing directly forms a hollow filament, often with an ionic or photochemical crosslinking step. Light-based printing can pattern fine channels at high resolution, while microfluidic printing can impose coaxial geometry or material gradients. Each must balance skin-scale coverage with microvascular-scale transport.

Post-print self-organization complements imposed geometry and dynamic culture.[32,81] A gelatin/GelMA/oxidized-dextran system organized endothelial and smooth-muscle cells into separate layers, but its ischemic-hindlimb perfusion and skin-wound fibroblast-persistence results came from separate anatomical experiments.[82] Neither result supplies the missing measurement in the other model.

A hybrid coaxial/extrusion approach produced "small-micro" vascular networks in GelMA skin substitutes; red dye filled S-shaped and grid lumens within seconds, and 40-kDa fluorescein–dextran transport was imaged post-injection.[18] A biopsy-sized skin model with a perifollicular plexus directly perfused ink, dextran, and living T cells through its network for immune-trafficking studies, but was not a wound-repair or transplantation model and did not demonstrate host integration.[20] A perfusable skin-on-chip used defined channels and pump-driven transport of 4-

and 70-kDa dextrans during specified assay intervals in a controlled device.[21] Free-standing constructs prioritize graft architecture; chips offer controlled flow and assays; these require separate comparison.

Basic studies provide design precedents. Miller *et al.*[83] first printed carbohydrate-glass templates, cast cell-containing matrices around them, and removed the templates, demonstrating channel flow, subsequent endothelial lining, and improved cellular function compared with slab constructs. Kolesky *et al.*[84] combined sacrificial and cell-laden printing with casting to produce gelatin–fibrin tissues with endothelialized channels, including pump perfusion, permeability measurements, and a separate 30-day osteogenic differentiation demonstration. These non-skin studies establish fabrication and transport principles; the long-duration vascular and thick-tissue differentiation experiments should remain distinct when compared with a skin graft.

As a contextual fabrication example, Kim *et al.*[85] combined pre-set coaxial extrusion of skin-derived decellularized matrix with endothelial sprouting induced by a biochemical gradient. Injected fluorescent particles passed through lumens and branches. This links designed channels with sprouting, but the construct was not a transplanted dermo-epidermal graft; sustained flow, endothelial-barrier performance, and host access require separate tests.

High-resolution, microfluidic, and microgel platforms, VesselNet, and surgically connectable flap systems provide contextual strategies for scale bridging.[86-90] Their results concern their tested tissues and connections; they are not additional demonstrations of vascular integration in bioprinted skin.

Skin chips can test inflammation, edema, and microvascular-epidermal interactions under controlled operation.[91,92] Device-supported function remains distinct from post-transplant access to host circulation.

Direct lumen filling is informative when its temporal limits are retained. In a digital-light-processing model, endothelial capillary-like structures were tested after seven days of culture. A micropipette was inserted into one end of a tube, and the distal end was cut before fluorescein was injected at 150 hPa for 1 s. Dye then propagated along the lumen. Figure 3 reproduces this transient patency assay. The authors distinguished it from robust, continuously connected microfluidic perfusion, which remained to be established. The observation is therefore described as injection-assisted lumen passage under the reported pressure and duration. The model was neither printed skin nor a chronic-wound treatment.[93]

Transport measurements can then be used to determine if a patent pathway alters the surrounding tissue environment. In cell-laden silanized hydroxypropylmethylcellulose constructs, sacrificial gelatin was removed to form channels, which were then perfused with culture medium at 0.5 mL/min. Central oxygen concentration fell when flow stopped and recovered when flow resumed, as shown in Figure 4. This controlled perturbation links perfusion to oxygen availability. The channels were not endothelialized, and skin repair or host integration was not tested. The study therefore provides an assay principle for tissue transport, not evidence of a mature skin vasculature.[94]

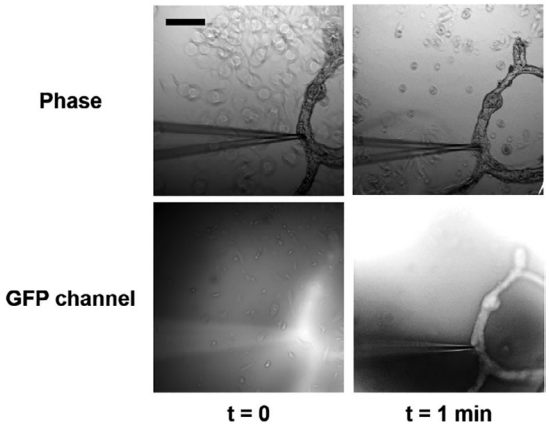

Figure 3. Transient microinjection demonstrates lumen passage, not sustained network perfusion. Endothelial progenitor-cell tubes were tested after 7 days of culture. The pipette entered one end of a tube, and the opposite end was cut. Fluorescein injection used 150 hPa for 1 s; a flow rate was not quantified. The original panels show $t = 0$ and $t = 1$ min after dye microinjection, with a 100-µm scale bar. Phase denotes phase-contrast imaging; GFP is the original green-fluorescence-channel label. This non-skin platform supports injection-assisted patency; persistence of vascular morphology over longer culture periods does not demonstrate continuous flow. Reproduced from Mazari-Arrighi *et al.*[93] Copyright © 2024 The Authors. Licensed under CC BY 4.0. The complete original image was extracted from the publication PDF; scientific content is unchanged.

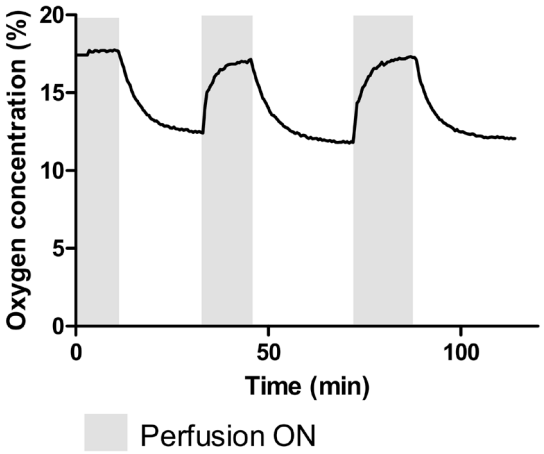

Figure 4. Flow interruption and restoration change central oxygen concentration. The original representative trace was measured in a 2% silanized hydroxypropylmethylcellulose construct containing primary ovine bone-marrow stromal cells at 8 million cells/mL and sacrificially formed microchannels. Perfusion was applied at 0.5 mL/min; shaded intervals denote perfusion on. This intervention supports a flow-dependent transport effect in a non-endothelialized, non-skin construct. The displayed trace is not a pooled mean, and a separate replicate count for this on/off trace was not specified. The central probe does not by itself establish endothelial lumen-specific oxygen delivery. Reproduced from Figueiredo *et al.*[94]

Porosity and vascular channels require separate interpretation. Sacrificial gelatin microparticles can increase solute transport in thick constructs, but a porous interstitium is not an endothelial lumen. Static and perfused comparisons provide evidence about flow and porosity, although the reported perfused-construct experiment was not a fully matched 2 × 2 design and therefore does not fully isolate their independent contributions.[95] Multiscale volumetric printing combines designed architecture with phase-separation-derived porosity; multiple pore scales alone do not demonstrate vascular integration.[96]

Table 2 compares representative direct-function observations and their assay limits. Cross-platform comparisons require the assay, observed flow duration, compartment, and endothelial source to remain explicit.

Table 2. Selected direct-function assays and the limits of their vascular claims

Study/model	Direct observation	Separate time and operation fields	Assay description	Attribution and limitation
Luo *et al.*;[18] unimplanted printed skin	Dye and 40-kDa dextran passage through defined lumens	Assessment time: Dye: age NR. Dextran: culture day 14. Flow/injection condition: Slow syringe injection; dextran 1 mg/mL; rate/pressure NR. Observed flow/access interval: Dye fills within 10 s; dextran images 0/10/20/30 min. No uninterrupted-flow record.	Injection-assisted channel patency	Channel patency, not host integration. PDF p16, Fig4; p20.
Shah *et al.*;[20] unimplanted skin/follicle model	Ink, dextran, and T-cell passage in perifollicular vascular network	Assessment time: 5–7 d ALI before analysis; assay age NR. Seeding-order discrepancy. Flow/injection condition: Culture 0.5 then 2.4 mL/min; ink injection; tracer-specific rate NR. Observed flow/access interval: Dextran images every 5 min, to 60 min; T-cell windows to 15 min. Not culture duration.	*In vitro* network passage	Functional modeling platform, not wound-repair efficacy. PDF pp5–8, Figs1,2,4.

(*Cont'd...*)

Table 2. (*Continued*)

Study/model	Direct observation	Separate time and operation fields	Assay description	Attribution and limitation
Maggiotto *et al.*;[21] unimplanted printed skin chip	Pumped 4- and 70-kDa dextran transport	Assessment time: EC characterization day 21; device-tracer assay age NR. Flow/injection condition: Culture 10 then 30 μL/min; 70-kDa tracer at 30 μL/min. Observed flow/access interval: 4-kDa tracer: 15 min; 70-kDa images every 30 s for 30 min. Separate from culture/follow-up.	Pump-supported transport; permeability tested separately	Device-supported transport does not establish host inosculation. Sections 2.12–2.14, Figures 2 and 6.
Mazari-Arrighi E *et al.*;[93] non-skin EC platform	Fluorescein microinjection through endothelial tube after distal cut	Assessment time: Culture day 7. Flow/injection condition: Distal cut; 35-hPa compensation; 150 hPa for 1-s injection. Observed flow/access interval: Snapshots at 0 and 1 min after injection; continuous tracking interval NR. Neither culture age nor injection setting is sustained-flow duration.	Transient microinjection patency	Transient injection-assisted patency only. Continuous perfusion not established. PDF pp. 5–7, Figure 5.
Figueiredo *et al.*;[94] non-skin cell-laden channel	Central oxygen responds to pump on/off in printed sacrificial channels	Assessment time: Oxygen profiles at 24 h; pump-cycle trace age not separately reported. Flow/injection condition: 0.5 mL/min; deliberate pump stop/restart. Observed flow/access interval: Continuous oxygen trace across interrupted pump cycles; response times are not uninterrupted-flow duration.	Pump-supported transport without endothelial lining	Direct oxygen measurement; no endothelial barrier. Main-text numerical inconsistency noted. PDF p6, Figure 3.
Dudaryeva *et al.*;[96] non-skin vascular chip	Main-channel perfusion plus cellular outgrowth in porous matrix	Assessment time: 1-wk preculture; outgrowth at 2 wk total culture. Flow/injection condition: Reported 1-wk pump operation: 300 μL/min for 2 d, then 700 μL/min. Observed flow/access interval: Direct flow-tracking duration NR. Operation schedule and outgrowth do not prove all sprouts carry flow.	Reported sustained main-channel operation; direct tracking interval separate	Perfused main channel does not prove every capillary-like sprout carries flow. PDF pp. 8–11, Figure 4.
Hudson *et al.*;[95] non-skin collagen tube	Printed collagen tube patency with surrounding cast-cell viability	Assessment time: Methods/results: 10 d; Fig. 4C–E: 5 d. Source discrepancy. Flow/injection condition: Culture pump 220 μL/min; dye injection rate/pressure NR. Observed flow/access interval: Dye-patency snapshots; tracking interval NR. The 5/10-d conflict concerns culture/viability.	Pump-supported tube transport without endothelial lining	Oxygen distribution is simulated, not directly measured. Not a full matched 2 × 2 design. PDF pp. 3–7, Figure 4.
Baltazar *et al.*;[22] implanted printed skin graft	Host-injected UEA-I accesses human endothelial-lined vessels	Assessment time: 4 wk post-graft (Figure 6); adjacent histology also termed 30 d. Flow/injection condition: 200 μL tail-vein UEA-I, 1:1 saline; 30-min circulation before harvest. Observed flow/access interval: Terminal section-based access after 30-min circulation; no continuous-flow recording.	Source-resolved host tracer access	Source-resolved graft blood access in acute immunodeficient mice. PDF pp. 4,6,9, Figure 6.

(*Cont'd...*)

Table 2. (*Continued*)

Study/model	Direct observation	Separate time and operation fields	Assay description	Attribution and limitation
Baltazar *et al.*;[23] implanted xeno-free skin graft	Infused Ulex plus human/mouse CD31 distinguishes graft and host vessels	Assessment time: Separate terminal assessments at 2, 4, and 6 wk. Flow/injection condition: 200 µL of 1 mg/mL UEA-I; 30-min circulation before harvest. Observed flow/access interval: Terminal access at each time point; no continuous 6-wk flow record.	Source-resolved host tracer access	Acute immunodeficient model, not chronic clinical integration. PDF p9, Figure 6.
Vuerich *et al.*;[97] non-printed ischemic skin wound	Intravenous lectin enters donor/host hybrid vessels	Assessment time: Day 7 postimplantation. Flow/injection condition: 5 µg IV lectin 10 min before sacrifice. Observed flow/access interval: Terminal donor/host access after 10-min circulation; continuous-flow recording NR.	Source-resolved host/donor access	Disease-relevant tracing comparator, not proof of bioprinting benefit. PDF pp. 10–13, Figure 6.
Fischer *et al.*;[98] non-skin printed muscle flap	Femoral arterial connection and blood entry; terminal vascular cast	Assessment time: Immediate clamp release; terminal cast day 14. Flow/injection condition: Femoral anastomosis; saline then Microfil at terminal harvest; rate/pressure NR. Observed flow/access interval: Immediate macrovessel blood entry and day-14 anatomy; continuous graft-flow duration NR.	Surgical macroconduit blood entry; terminal anatomy	Non-skin macrovascular evidence; whole-limb flow and terminal cast do not isolate longitudinal microvessel flow. PDF pp. 8–9, Figures 4–5.

Notes: The table presents selected primary experimental studies for qualitative comparison, including printed skin models and non-skin and non-printed comparators. Assessment time points, experimental operating conditions, and observed flow or tracer-access intervals are reported separately. NR indicates information not reported in the source examined; unavailable supplementary materials are documented separately in the source log. Discrepancies in cell-seeding order (Shah *et al.*[20]) and assessment time points (Hudson *et al.*[95]) are identified in the corresponding entries. Injection-assisted channel patency, pump-supported transport, endothelial barrier function, and host-derived tracer access represent distinct experimental outcomes. No pooled analysis was performed. Page, figure, and section references refer to the original publications.
Abbreviations: ALI: Air–liquid interface; CD31: Cluster of differentiation 31; EC: Endothelial cell; IV: Intravenous; NR: Not reported; UEA-I: *Ulex europaeus* agglutinin I.

5.3. Separate patency, perfusion, and endothelial barrier assays

A patency experiment requires a defined lumen and direct observation of fluid or tracer passage under a stated injection or flow condition. A sustained-perfusion claim additionally requires the measured duration of flow, with inlet/outlet configuration and flow rate or pressure reported. Hydraulic resistance, leakage, and tissue transport can be measured as separate attributes. An endothelial-barrier claim requires identified endothelial coverage and permeability measurements with appropriate tracer sizes and controls. Endothelialized channels should be compared with channels lacking an endothelial lining; the latter may lie within a cell-laden construct and are not necessarily wholly acellular. Flow direction and the interval actually observed should accompany every assay.

Cell viability under perfused culture conditions is a separate outcome. Medium circulation around dense collagen constructs has been shown to increase construct viability, but this observation alone does not establish intraluminal vascular flow.[52] Authors should indicate the nature of the space that is being perfused (printed channel, self-assembled lumen, porous bulk matrix, or external compartment in an engineered chip). Attribution to an endothelial barrier requires an endothelial lining and is strengthened by quantitative permeability measurements across multiple tracer sizes.

A custom bioreactor supported perfusion of non-skin myoblast constructs, but its culture and computational nutrient-distribution results do not establish skin-graft

vascular function.[99] For skin, hardware operation must be evaluated together with endothelial and epidermal barriers.

Hybrid skin models separate mechanical support from endothelial barrier assessment. Wu *et al.*[100] cast fibroblast-laden GelMA into melt-electrowritten polycaprolactone scaffolds and incorporated a separate endothelial cell-associated tubular insert. Medium passage through the insert was reported, with its direct demonstration provided in a supplementary video accompanying their article. A non-printed collagen/keratin model used a needle-templated channel and rocker-driven culture, measuring leakage of injected 70-kDa dextran; the blend reduced vascular permeability relative to collagen alone.[101] Reinforcement chiefly addresses mechanical patency, whereas dextran leakage interrogates vascular barrier performance.

Perfusion should be tested under failure-relevant conditions—start/stop cycles, handling, bending, compression, storage—and, for chronic wounds, glucose, cytokines, hypoxia, proteases, and bacterial products should be included. The vascular network needs to remain open during epidermal barrier formation to ensure optimal performance of one compartment without compromising the other.

6. From implantation to host integration

Host access has different roles in the products described in Section 8.2. A bioactive dressing may promote recipient repair, whereas a prevascularized graft requires source-resolved access to its vascular compartment. Designed-channel constructs also require assessment of their connection to the recipient circulation.

6.1. Host angiogenesis is not host–graft inosculation

After implantation, at least four vascular events can occur: host vessels grow towards the implant, host vessels invade the matrix, graft ECs form vessels, and host circulation gains access to graft-associated lumens. Histological host CD31-positive vascular density supports angiogenic activity but does not establish the last event. Source-resolved host access requires blood or a circulating tracer within a defined graft-associated lumen, with donor or host endothelial identity resolved by suitable labels. Regional wound blood flow concerns a different compartment. Structural contact or a junction image alone does not demonstrate flow continuity. An access assay establishes access at its sampled time point and must not be described as durable perfusion without longitudinal functional evidence.

Source-specific tracing distinguishes host access from vascular histology in the selected skin studies. In a four-cell graft, *Ulex europaeus* agglutinin I and mouse lectin distinguished human and mouse vessels; tail-vein tracer identified human-lined graft vessels accessed from host circulation, and reported anastomosis.[22] In the xeno-free graft, host-injected fluorescent lectin reached human CD31-lined vessels, showing circulation access; ECs and pericytes reduced early necrosis versus a nonvascular control.[23] Spatially patterned primary or iPSC-derived networks underwent direct pre-implantation perfusion, and host-circulating rhodamine–dextran later marked graft vessels; spatial overlap supported integration but did not prove blood traversed the human channel or reveal a human–mouse junction.[60] Host-injected tracer plus source labels support stronger attribution than marker-only histology; localization to the graft region without source-specific colocalization supports a weaker claim.

The robotic substitute and flexible flap platform illustrate distinct routes of vascular integration. In the robotic substitute, human–rat CD31-positive vascular connections and recipient rat erythrocytes within human endothelial-lined lumens provided histological evidence that host blood reached graft vessels at the sampled time point (Supplementary Figure S2b–c of Pontiggia *et al.*[80]). Although assessments were conducted 1–3 weeks after implantation, the precise timing and biological replication of the supplementary observations were not specified, and the duration of continuous graft perfusion was not reported. In the flexible flap platform, surgical anastomosis to the femoral vessels enabled immediate but incomplete blood filling of a printed tubular scaffold.[90] However, this observation does not establish equivalent perfusion in the final folded skin flap, for which the available evidence primarily comprised *in vitro* perfusion and histological evidence of tissue ingrowth.

Figure 5 illustrates source-resolved host-circulation access in xeno-free bioprinted skin grafts. For infused Ulex, the results were correlated with human and mouse CD31 staining at two, four, and six weeks. The paired labels are used to distinguish between host vessel recruitment, nonperfused human ECs, and graft vessels accessed by the host circulation. It is a more compelling finding than staining alone, but it is an immunodeficient implantation model, not a demonstration in a chronic human wound.[23]

Contextual studies of endothelial-coated microspheres, microgel tissues, VesselNet, and non-printed prevascularized skin examine spontaneous or surgical host connection.[67,88,89,102] The muscle-flap conduit experiment separately documented immediate blood entry and a day-14 terminal vascular cast; neither observation measures longitudinal flow through a printed skin microvascular

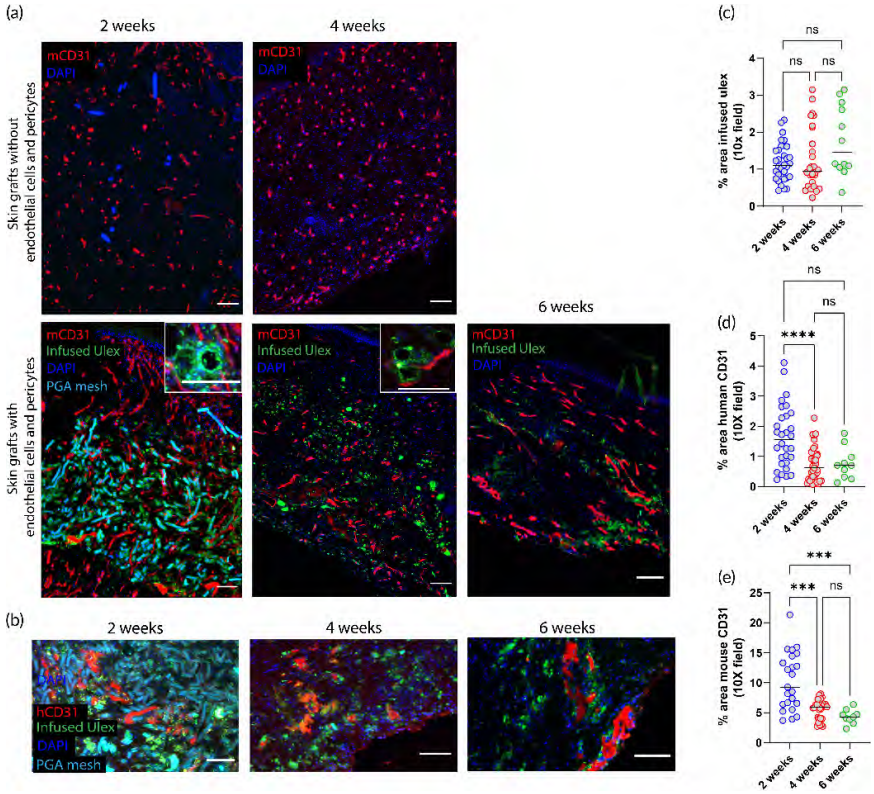

Figure 5. Host-circulation access and endothelial source in xeno-free bioprinted skin grafts. Grafts containing endothelial cells (ECs) and pericytes (PCs) were assessed 2, 4, and 6 weeks after implantation in immunodeficient mice. EC/PC-negative comparators are shown at 2 and 4 weeks. (a) Mouse CD31 staining identifies host angiogenesis (red), while infused Ulex labels perfused human EC-lined vessels. (b) Human CD31 staining combined with circulating Ulex distinguishes nonperfused human ECs (red) from infused-Ulex-positive human vessels (green). Nuclei are blue after DAPI (4′,6-diamidino-2-phenylindole) staining; the polyglycolic acid mesh autofluoresces in blue/green channels and appears cyan at 2 weeks. Scale bars: 100 μm. Quantified areas are shown for (c) infused Ulex, (d) human CD31, and (e) mouse CD31. The source reports three independent experiments and one-way analysis of variance with Tukey comparisons: *$p < 0.05$, **$p < 0.01$, ***$p < 0.001$, ****$p < 0.0001$; ns, $p > 0.05$. This experiment supports source-resolved host access, not chronic human-wound efficacy. Reproduced from Baltazar *et al.*[23] Copyright © 2022 The Authors. Licensed under CC BY 4.0.

compartment.[98] These comparisons identify connection strategies, not interchangeable skin-graft outcomes.

Non-printed skin comparators further show the importance of source localization. A cast prevascularized skin component combined with printed cartilage contained rat erythrocytes within human endothelial lumens, whereas increased regional AngioSense signal in a plasma-gel substitute did not identify the endothelial source of the accessible compartment.[103,104] Neither skin component was bioprinted.

An ischemic-wound comparator shows why cell-origin resolution matters. A non-printed stromal vascular fraction study combined donor-source labeling with intravenously administered lectin. At day 7, lectin-accessible vessels contained both host and donor endothelial contributions, supporting a hybrid-vessel mechanism. The transferable contribution here is donor-resolved tracing; the study did not test a bioprinting advantage.[97]

6.2. Integration must be durable and physiologically useful

A single early tracer image demonstrates vascular access only at the sampled time point; it is not sufficient to establish durable function. Persistent patency, adequate flow distribution, controlled permeability, maturation and survival of the overlying tissue are required for clinical function. Vessel density alone cannot establish whether flow is adequately distributed. Excessive vascular leakage may worsen edema. Inadequate pericyte support may destabilize a network, but greater pericyte investment is not by itself evidence of abnormal remodeling. Mural-cell identity and coverage, including α-SMA-positive cells, must be interpreted with vessel caliber and anatomical context.

A well-designed longitudinal study should measure the percentage of graft vessels perfused, the percentage of graft vessels connected to host vessels, the extent of penetration

from the wound edge, the distribution of vessel caliber using an objective technique, and the survival of ECs from the graft versus host. Lineage or construct localization might be useful in combination with multiphoton imaging, intravital microscopy, contrast ultrasound, micro-computed tomography angiography, photoacoustics, or repeated laser-speckle imaging. Histology at the end of the study should relate regional flow to endothelial source and tissue survival.

Additionally, there is an issue of hemocompatibility with anastomosis. Evidence of connection should be included along with thrombosis and inflammatory injury in the vascular evaluation. Anti-thrombotic conditioning, platelet deposition, coagulation, extravasation of red cells, and leakage of vessels should be studied. Burst pressure and suture retention are important with surgically connected conduits, while speed of inosculation and ischemic interval prior to connection are important with microvascular self-assembly.

6.3. Vascular access also exposes grafts to immune surveillance

The engineered endothelium serves not only as a transport interface but also as a regulator of graft immunogenicity. Using a humanized-mouse model of printed skin, Tobiasova *et al.*[105] demonstrated that major histocompatibility complex (MHC) expression by ECs contributed to T-cell-mediated rejection. Grafts containing ECs lacking both MHC class I and class II showed minimal T-cell infiltration and no observed rejection during follow-up. These findings highlight the immunological implications of incorporating endothelial cells into engineered skin constructs. Although the study demonstrated vascular structures within the grafts, it did not independently establish sustained graft perfusion. Thus, its principal contribution concerns graft immunobiology rather than direct validation of vascular flow.

Complementary skin models isolate immune-transport questions: printed-channel fibrin equivalents measured injected monocyte recruitment, while an endothelialized skin chip combined permeability testing with neutrophil perfusion and interleukin-8 blockade during viral infection.[106,107] These are controlled *in vitro* observations; implanted-graft survival and chronic-ulcer efficacy require separate tests.

Ahmed *et al.*[108] manufactured donor-matched, bioprinted human skin equivalents for antibody-challenged immune co-culture and detected treatment-dependent proinflammatory cytokine responses. This provides a complementary model for immune-response testing, while vascular transport, implanted-graft persistence, and chronic-wound efficacy require separate evaluation.

This distinction is relevant in selecting cells. Autologous cell origin, immunomodulation, and vascular maturity should not be regarded as interchangeable or universally sufficient strategies for mitigating graft-related risks. After inflammatory activation, ECs may be lost from a graft that passes a short-term patency test. Conversely, reducing endothelial immune signaling requires assessment of host defense and surveillance, in addition to graft persistence. Immune compatibility is therefore an important factor in disease-relevant flow tests, along with transport and barrier integrity, and tissue survival. These are proposed qualification questions, not evidence of a clinically proven immune-evasion strategy.[16,105]

7. Disease-oriented wound repair and chronic-ulcer relevance

7.1. Fresh wounds in diabetic models and clinical diabetic foot ulcers

Four core studies investigated newly created wounds in diabetic animals, whereas one examined human diabetic foot ulcers. In the all-peptide study, 10-mm wounds were created in rats 3 days after STZ administration (70 mg/kg) and treated immediately.[40] This model therefore evaluated the repair of acute wounds in diabetic animals rather than established nonhealing ulcers. Although histological examination revealed vascular structures, whole-wound laser speckle contrast analysis assessed regional blood-flow signals without specifically demonstrating perfusion through printed vessels.

The curcumin–GelMA–ADSC construct addressed oxidative injury and measured wound vascular markers.[19] The collagen DLP construct measured wound vessel morphology and morphometry.[39] The photosynthetic scaffold used an independent HUVEC/Matrigel tube-formation assay rather than demonstrating an endothelialized printed channel; wound CD31 staining and oxygen-related outcomes were separate observations.[28] The clinical adipose-tissue/fibrin series reported no vascular assay.[109] Cell protection, host repair, and clinical coverage therefore remain distinct from demonstrated flow through a printed vascular compartment.

Table 3 distinguishes wound history, treatment product, repair outcomes, and the anatomical compartment assessed for vascular function. Clinical-ulcer observations are presented separately from findings in newly excised animal wounds, without pooling their outcomes.

7.2. A broader chronic-wound toolbox

Recipient-bed interventions supply context for the direct

Table 3. Wound history, repair outcomes, and vascular attribution

Study	Model/sample	Intervention	Reported outcome	Vascular boundary
Bajuri *et al.*[109]	Clinical diabetic foot ulcers; *n* = 10; single arm; pre-enrollment ulcer duration NR	Autologous minimally manipulated adipose tissue + fibrin	7/10 fully epithelialized by week 12; remaining area reduced 83%, 96%, and 86%	No vascular endpoint; no comparator; limited follow-up. Closure does not establish vascular function.
Xia *et al.*[19]	Fresh 15-mm splinted excisions in STZ-treated nude mice; 30 mice total; endpoint-specific n NR	10% GelMA + 20 μM curcumin + human ADSC	Improved closure/re-epithelialization; day-21 DiR signal retention; exact closure percentages NR	CD31/α-SMA markers only; no lumen or flow assay; total implant curcumin dose/release/safety incomplete.
Huang *et al.*[40]	Fresh 10-mm excision after STZ 70 mg/kg; Methods: 3 d later, immediate treatment; 82 rats main + 30 splint study	PGA-SH/PGA-GMA peptide hydrogel + VEGF165-overexpressing HUVEC	Faster closure and re-epithelialization; greater wound-region perfusion signal	Wound vascular structures with unresolved endothelial source. LASCA measures whole-wound flux, not printed-vessel flow. Pre-treatment nonhealing not established.
Wang *et al.*[28]	Fresh 10-mm excision in STZ-treated mice; *n* = 8/group; no established pre-treatment nonhealing period reported	Microalgae/GelMA–alginate hollow scaffold	Less residual wound area and greater CD31 staining; light-versus-dark closure difference was not established	Independent 6-h HUVEC/Matrigel tube assay outside the printed channel. Wound CD31 is separate; channel perfusion and microbial clearance NR.
Fu *et al.*[39]	Fresh paired 9-mm excisions after 3 weeks of qualifying hyperglycemia; *n* = 15/group; 60 diabetic + 5 nondiabetic rats	Collagen methacrylate + 0.01% DHM + HDF	>85% closure by day 10 and near-complete healing by day 18; vessel diameter/density increased but exact means NR	Wound vascular morphology; no EC in the treatment construct. Control infection and paired-wound analysis unclear.
Jorgensen *et al.*[17]	Acute nude-mouse wound; *n* = 4/group	Three-layer, six-cell printed skin	Earlier epithelialization and more normal collagen organization; not increased contraction	ZO-1-positive lumens; no blood tracing or EC-specific fate tracking.
Vuerich *et al.*[97]	Ischemic mouse wound; *n* ≥ 3/group; total animals NR	Non-printed stromal vascular fraction	Lectin-accessible host–donor hybrid vessels and improved repair	Source-resolved host/donor tracer access in an ischemic wound comparator; not bioprinted skin.

Notes: The table presents selected primary studies for qualitative comparison; no pooled efficacy analysis was performed. Wound chronicity was classified according to documented preintervention wound history rather than underlying disease status alone. Sample sizes refer to the reported study populations and may differ from endpoint-specific denominators. NR indicates information not reported in the cited source. DiR fluorescence indicates retention of the cell-labeling signal rather than directly confirming donor-cell survival.
Abbreviations: ADSC: Adipose-derived stem cell; CD31: Cluster of differentiation 31; DHM: Dihydromyricetin; DiR: Lipophilic near-infrared fluorescent carbocyanine dye; EC: Endothelial cell; GelMA: Gelatin methacryloyl; HDF: Human dermal fibroblast; HUVEC: Human umbilical vein endothelial cell; LASCA: Laser speckle contrast analysis; NR: Not reported; STZ: Streptozotocin; VEGF165: Vascular endothelial growth factor A isoform 165; ZO-1: Zonula occludens-1; α-SMA: α-smooth muscle actin; γ-PGA-GMA: Glycidyl methacrylate-conjugated poly(γ-glutamic acid); γ-PGA-SH: Thiolated poly(γ-glutamic acid).

wound studies in Table 3. Refractory-ulcer substitutes, antioxidant bioinks, antibiotic scaffolds, microalgae, or vesicle dressings and oxygen-sensing grafts target different constraints, including inflammation, infection, oxygen availability, and matrix repair.[30,31,41,42,70,71,110,111] Their relevance is to complementary wound management; they do not replace construct-localized vascular measurements.

A mismatch between the repair quality and gross wound closure may occur even if an angiogenic payload is used. Handheld printing of vascular endothelial growth factor-loaded GelMA increased wound-bed von Willebrand factor staining and several epithelial and scar-related parameters at day 14 in acute porcine wounds, but there was no significant difference in gross wound closure.[112] A separate study evaluated growth-hormone-loaded, printed carboxymethylcellulose–silk fibroin dressings in diabetic ischemic rat wounds. In selected treatment groups, tissue organization and CD31-associated microvessel density were enhanced, and there were no significant differences in wound closure rates at any time point during the 14-day

follow-up.[113] The two studies concern distinct recipient beds and cell-free delivery systems. They warrant remodeling assessment in addition to closure, with vascular histology reported separately.

Multilayer polyurethane/bioglass patches and a DLP bilayer burn system illustrate fluid handling, barrier, and repair functions.[114,115] In the latter, infected-wound and keratinocyte-containing treatment arms must remain separate. These studies inform surface protection rather than demonstrate blood flow through graft vessels.

Non-printed materials offer additional comparators for these specific functions. Glucose-responsive chitosan nanohydrogels address metabolic and infection-related conditions; alginate/sericin films with polysaccharide-capped silver nanoparticles address infection control; and electrospun chitosan/polyvinyl-alcohol/polyethylene-glycol/nonwoven membranes address dressing compatibility and fluid handling.[116-118] These sources are used qualitatively at the material level. They do not establish perfusion of an endothelialized printed compartment or graft-specific access to host circulation.

Recipient-bed dependence is also evident in non-printed fibroblast/endothelial-progenitor spheroids whose effect differed with the timing of irradiation.[119] A portable-printer pilot in compression-induced ischemic pig wounds supplies procedural and histological experience through day 36, but its single-animal design does not provide independent animal-level efficacy replication.[120]

A prospective study could compare the same construct across healthy acute wounds, fresh wounds in disease-background animals, and established nonhealing wounds. For products intended to carry flow before implantation, separate patency, sustained-perfusion, and endothelial-permeability assays would describe baseline hydraulic and barrier properties. After implantation, circulating tracers localized to graft-associated lumens with source labels would assess host access; repeated functional observations would assess persistence. Wound-level perfusion, closure, epithelial barrier, infection control, and scarring should be measured separately. A composition-matched nonperfusable construct would help test whether flow contributes beyond bioactive cargo. This is a proposed validation design, not evidence already established in chronic ulcers.

7.3. Large animals and human observations are necessary but not self-validating

Large-animal *in situ* printing provides evidence relevant to scale, anatomical handling, and autologous-cell workflows. Autologous skin-cell printing accelerated healing of large wounds in pigs, and the cited *in situ* systems were tested across mouse, rat, and porcine models.[26,27] Complementary studies evaluated samples from large bioprinted dermo-epidermal substitutes in immunosuppressed mice and intraoperative adipose-cell printing in immunodeficient rats.[121,122] These studies examine coverage, reconstructive logistics, or acute repair. Construct scale, recipient species, and human use are applicability descriptors; none substitutes for measured graft-specific vascular function or demonstrates durability in a chronic ulcer.

Human wound-healing observations are clinically relevant even when the vascular mechanism is unmeasured. The single-arm diabetic-foot-ulcer series provides feasibility and closure observations, but no vascular endpoint, no comparator, and no reported baseline ulcer duration.[109] It cannot establish that the printed adipose–fibrin product formed a functional vascular network. Future clinical studies would need clinically justified measurements of implant-localized vascular function, safety, durability, recurrence, and comparison with standard care. These requirements describe unresolved questions, not conclusions supplied by the present clinical series.

Other adipose/fibrin reports concern acute defects after skin-cancer excision and limb salvage in one patient receiving vascular and surgical care.[123,124] They provide clinical workflow observations, not comparative efficacy or attribution of repair to a patch-specific vascular network. Angioplasty, debridement, antibiotics, and subsequent care remain important cointerventions.

8. Translation and clinical readiness

8.1. Match the manufacturing route to the clinical product

Bioprinted skin can be manufactured as a matured graft, printed directly *in situ*, or supplied as a device-assisted procedure. The vascular strategy is modified in each route. A matured graft can undergo pre-implant perfusion and release testing where compatible with the product design, but also requires culture time, transport, sterility assurance, and surgical fixation. Conforming to an irregular wound and minimizing transport-related damage to fragile tissue may be possible with *in situ* printing, but the deposited network may not have preformed flow and may need to endure an ischemic interval. Commercial hardware alone does not validate the biological product. Nevertheless, handheld and multi-degree-of-freedom robotic systems can improve mobility and surface registration, while single-step epidermal bioinks may reduce culture complexity.[125-127]

The intended duration of clinical use determines the functional and handling requirements of the product. The reviews of living skin equivalents differentiate temporary

protection/replacement with host tissue from long-term maintenance of grafts, and identify the practical constraints of storage and handling of the living skin equivalents, the cellular composition, or cost.[128] There are also distinctions in the understanding of removable coverings versus permanent replacements in the categories of adhesion and moisture control made by Oualla-Bachiri *et al.*[129] These needs overlap with host biology: Kondej and colleagues[130] discuss immune responses and tissue integration; Sörgel and colleagues[131] discuss speed of vascularization and manufacturing time and cost of bioprinted substitutes. These are complementary design views and not alternative clinical outcome sets. They collectively contribute to the determination of the target wound, the process to be applied, and the duration of the product, before deciding on a vascular strategy or its release assay.

The term *scalable* must be measured in clinically meaningful terms and time. A good print at biopsy size is not necessarily going to be uniform over tens or hundreds of square centimeters. Long fabrication times can introduce differences in material conditions and cell exposure between printed layers, whereas extrusion parameters influence shear exposure. Extended tool paths may also contribute to within-batch variability. Furthermore, photopolymerization depth can vary along the wound around the contour. Different avenues for skin regeneration include micro–nano porous scaffolds, lipoaspirate-derived constructs, skin organoids, adipose-stromal-cell substitutes, and fish-skin-based GelMA. Their scalability, batch consistency, and vascular release requirements remain to be demonstrated for the intended clinical product.[48,66,132-134]

Surface registration, tool orientation, and the biological impact of bioink deposition are additional considerations for the feasibility of intraoperative bioprinting. In a pilot study, a six-axis robotic bioprinter was adapted to scan and print directly onto porcine burn wounds following debridement on day 7 after burn induction.[135] Fibroblast-containing bioink was compared with cell-free bioink and 1% silver sulfadiazine, with wound healing and scar formation monitored through 42 days after burn induction. The study demonstrated the feasibility of integrating robotic bioprinting into surgical workflows involving living, potentially moving tissue surfaces. However, all six wounds were created in a single pig, and vascular characterization was limited to supplementary histological findings. Larger studies involving independent animals are therefore needed to establish reproducibility and evaluate the relationships between printing performance, wound healing, and vascular function using direct vascular assessments.

8.2. Define critical quality attributes before clinical trials

Figure 6 illustrates manufacturing routes and the verification of host-to-graft circulation access to graft-associated vessels. Product identity, product-appropriate preimplant testing, disease relevance, clinical scale, and durable function are discussed in the surrounding text rather than depicted as a complete validation pathway in the figure. The illustration does not specify a uniform vascular approach and is not a regulatory requirement. The potency assays and claims for a cell-free dressing and a matured vascularized graft are different.

Critical quality attributes for a vascularized bioprinted skin product should go beyond viability and print fidelity. Material properties such as composition, polymer modification, residual crosslinker, degradation, swelling, stiffness, permeability, and batch variability must be defined. Cellular characteristics encompass identity, purity, passage, donor variability, potency, microbial status, and post-print viability. Structural attributes include layer thickness, channel continuity, diameter distribution measured using an explicitly defined method, endothelial coverage, mural-cell association, and epidermal barrier integrity. Functional vascular characteristics include pressure–flow response, tracer permeability, leakage, and duration of patency and response to inflammatory or thrombotic insult.

The potency assay should correspond to the proposed mechanism of action. A product claimed to be perfusable before implantation should be supported by a reproducible flow assay conducted in a clearly defined vascular compartment. A structurally prevascularized product intended to connect after implantation should have documentation of vascular identity and architecture prior to implantation. Then, the timing and duration of host blood access should be tested in a prospective manner. Alternatively, a proangiogenic dressing can be based on release kinetics and a validated endothelial-response assay, without making the assumption that it already contains an inherent network of perfusion. In addition to oxygen output, a living photosynthetic or microbial product requires containment, assessment of genetic or phenotypic stability, light-dose control where applicable, and stopping rules. Personalized autologous products require defined manufacturing timelines, minimum cell-yield requirements, release criteria for products derived from donors with suboptimal cell quality or yield, and contingency plans for clinical deterioration during production.

Using xeno-free materials and defined cells can reduce uncertainty associated with xenogeneic components, but

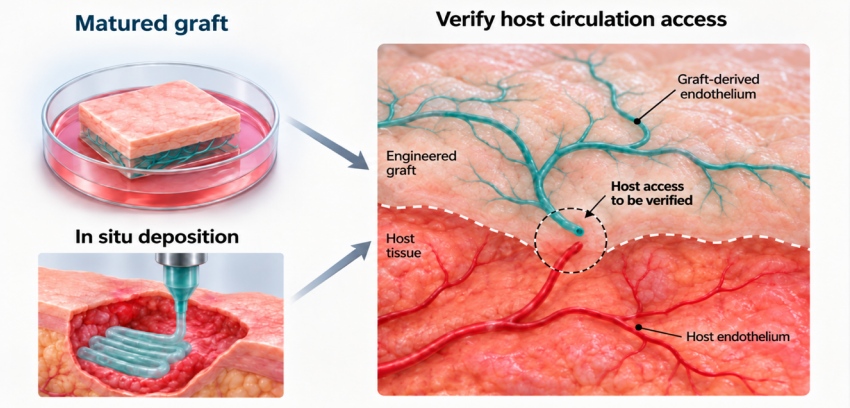

Figure 6. Manufacturing routes and verification of host–graft vascular access. *Ex vivo*-matured grafts and *in situ* deposition are illustrated as alternative manufacturing routes. In the enlarged interface view, blue-green and red vessels represent graft-derived and host endothelium, respectively; endothelial origin requires experimental verification. The white dashed line marks the proposed graft–host interface, and the separated vascular ends within the black dashed circle indicate host access to be verified, not an established anastomosis. Evidence of host-circulation access must be localized to graft-associated vessels, with the method and observation time stated. The representative vascularized construct does not imply that every *in situ*-printed product contains a preformed vascular network or that a matured graft is already perfused before implantation. Preimplant perfusion testing is product-dependent and is not a mandatory prerequisite for every graft to acquire host blood access. Disease-relevant testing, clinical scale, and durable function are discussed separately in Sections 8.1–8.3. Figure created by the authors with Adobe Photoshop. This is a conceptual illustration, not a regulatory standard; no experimental measurements are plotted.

does not eliminate allogeneic immune responses or other translational uncertainties. The xeno-free vascularized graft demonstrates that human plasma components, collagen, ECs, pericytes, fibroblasts, and keratinocytes could be integrated without using any animal-derived culture supplements, with engraftment demonstrated in immunodeficient mice. Donor sourcing, scale-up, and immune compatibility remain unresolved translational questions.[23] High-resolution fully biological collagen printing may lead to a reduction in the use of permanent synthetic material, but many questions remain about the process, including the mechanical aspects and the scale-up strategy.[53] Regulatory strategy should be initiated during bioink selection, and not after proof of concept.

8.3. Durable function remains an endpoint-specific question

The assembled evidence does not establish durable graft-specific perfusion in clinical chronic ulcers. Source-resolved access in immunodeficient implantation models demonstrates that host circulation can reach certain printed-skin vascular compartments, but the recipient bed, immune environment, and observation schedule limit translation. Repeated terminal tracer assessments at two, four, and six weeks are not continuous-flow measurements. Clinical closure without a vascular assay cannot fill that gap. This conclusion concerns the observations examined here and does not establish a field-wide absence of durable vascular function. Durability must be defined for a particular product, indication, and measurement interval.

Validation should follow the intended mechanism of the product. A construct designed for preimplant perfusion can be tested for sustained flow, pressure response, and endothelial permeability before implantation. A self-assembling graft may acquire flow only after host connection and requires a different assay schedule. In both cases, host access, source attribution, persistence, and tissue benefit must be measured separately in the intended recipient environment. Disease-matched models, immune compatibility, clinical scale, manufacturing consistency, and safety constrain applicability rather than define an evidence rank. Reviews support the need for maturation and clinically relevant testing, but those design priorities do not themselves demonstrate chronic-ulcer vascular integration.[1,3,4,12]

9. Minimum reporting set and research agenda

9.1. Report the printed system, not only the printer

Nozzle or optical resolution, pressure or energy exposure, speed, layer thickness, path, temperature, crosslinking chemistry and dose, dimensions of the constructs, and printing time should be given with each study. The composition of the bioink should include concentration, ratio, polymer modification, initiator, and all secondary crosslinks. Cell reporting should include source, donor number, passage, density, endothelial-to-support-cell ratio, and viability before and after printing. Reporting these parameters will facilitate independent replication of the vascular phenotype.

The final dimension of the model should be described with the thickness of each layer and overall dimensions of the model, rather than by a schematic or scale bar. The diameter of the vessels should only be reported if the authors have defined a measurement method and given numerical data. Scale bars are not measurements. In a hierarchical network, macrochannel, microchannel, and self-assembled capillary compartments should be reported separately, with dimensions and measurements attributed to the relevant compartment.

9.2. Match claims to vascular endpoints

A five-part endpoint reporting framework is recommended, comprising (i) vascular identity, including endothelial and supporting cell markers, source specificity, and junctional phenotype; (ii) vascular structure, including lumen continuity, diameter distribution, branch density, mural coverage, and basement membrane; (iii) *in vitro* vascular function, including inlet/outlet configuration, fluid and tracer characteristics, flow rate, pressure, permeability, leakage, and patency duration; (iv) *in vivo* integration, including host-circulating tracers, construct localization, endothelial source, anastomotic evidence, perfused fraction, and longitudinal persistence; (v) tissue outcomes, including graft survival, re-epithelialization, barrier function, closure, contraction, scarring, skin appendage formation, and recurrence.

Negative, inconclusive, or unconfirmed findings should be reported transparently rather than omitted. If a critical result is reported only in inaccessible supplementary information, it should remain unverified rather than be reconstructed from the prose text. For cases where animal number, group allocation, or denominator are not reported, "not reported" is preferable to an inferred sample size. Review articles should not be considered as "measurements."

A summary of practical claim-matched reporting requirements is provided in Table 4. Thresholds should be related to the product being developed and not simply taken from other tissue systems.

Table 4. A proposed claim-matched minimum reporting set

Claim or domain	Minimum information	Useful comparator/control	Interpretive boundary
Reproducible fabrication	Bioink concentration/ratio; cell source and density; crosslinker; energy/pressure; speed; layer geometry; print duration	Batch-to-batch and donor-to-donor repeats	Printer brand alone is not a reproducible protocol. [17,18]
Vascular identity and structure	Source-resolved EC markers; junctions; lumen continuity; explicit diameter method; mural association	Cell-free or vascular-cell-free construct	Positive CD31, ZO-1, or α-SMA is not sufficient evidence of flow. [17,19]
In vitro perfusability	Inlet/outlet; fluid and tracer; flow rate/pressure; duration; leakage; direction; repeatability	Composition-matched channel without endothelial lining; static/flow perturbation	Microinjection patency, continuous flow, and endothelial barrier are distinct. [18,93]
Improved tissue transport	Spatial oxygen or solute measurements; location; pump perturbation; viability at depth	Matched architecture and material, with and without flow	Modeled oxygen profiles are not direct measurements; absence of a matched control limits causal interpretation. [94,95]
Host–graft vascular integration	Host-circulating tracer or blood entry; construct localization; donor/host endothelial identity; time course	Nonvascularized graft; tracer-negative controls	Whole-wound blood flow and host angiogenesis do not by themselves establish graft-vessel perfusion. [22,23,97]
Chronic-wound efficacy	Disease induction/duration; wound depth and splinting; animal and wound denominators; closure; epithelialization; contraction	Disease-matched standard care and composition-matched construct	Acute immunodeficient models do not establish chronic-wound efficacy. [17,19,39,40]
Durable translational function	Longitudinal patency; barrier/leakage; tissue survival; inflammation; safety; recurrence; scale and manufacturing consistency	Clinically relevant comparator and duration justified for product	Large animals, human use, or a commercial printer alone do not establish durable graft-specific vascular function. [26,27,105,109]

Notes: This table presents a proposed minimum reporting framework based on the experimental evidence and assay distinctions discussed in this review. It is not a validated checklist, consensus guideline, or regulatory requirement. Quantitative acceptance criteria should be defined according to the intended product and clinical indication.
Abbreviations: CD31: Cluster of differentiation 31; EC: Endothelial cell; ZO-1: Zonula occludens-1; α-SMA: α-smooth muscle actin.

9.3. Link measured transport, host access, and tissue benefit

A useful experiment would connect angiogenic observations with spatially attributed functional measurements in the same construct before implantation where appropriate, during host access, and after remodeling. Composition-matched nonperfusable and vascular-cell-free constructs, together with disease-matched standard care, can help distinguish vascular contribution from material or cargo effects. *In vitro* fluid passage, sustained flow, endothelial permeability, source-resolved host access, and longitudinal tissue benefit should remain separate outcomes. Demonstrating one does not supply the others by inference. Clinically relevant wound history and follow-up are necessary to evaluate applicability to nonhealing ulcers.

Two key network-design requirements must be addressed: tissue exchange and vascular connection. Small, self-assembled capillaries provide an increased exchange surface area, but may take time to connect to circulation; large printed channels may allow pumping or surgical connection, but may leave diffusion gaps. With hierarchical designs, assess the communication between the levels and whether host blood does reach the smallest exchange compartment. Perfusable skin chips illustrate measurement of microvascular transport, while tissue-flap and VesselNet concepts illustrate engineering of macrovascular connection.[21,89,90] A clinically effective graft will likely need adequate exchange and access to a circulation; these examples do not imply that a skin chip itself must be incorporated into the graft.

Finally, studies should distinguish products containing vascular structures, products with experimentally demonstrated construct-specific perfusion, and products that promote host vascularization. Claims of construct-specific perfusion must be supported by direct evidence of flow within the construct. These product categories may provide clinical benefits through different mechanisms of action. Clearly defining each product's intended vascular function can guide experimental design, regulatory classification, and the formulation of appropriate clinical claims.

10. Conclusion

Vascular claims in bioprinted skin should specify the assay, measured compartment, endothelial source, observation time, model context, and construct relevance. The reviewed literature includes structural observations, injection-assisted patency, sustained device-supported transport, and source-resolved host-circulation access, with different model and construct boundaries. Selected printed-skin grafts demonstrate host access in immunodeficient implantation settings. Studies in freshly excised diabetic wounds provide evidence for repair and cell protection, while the clinical ulcer series has no vascular endpoint. These findings do not establish durable printed-vessel function in chronic clinical ulcers.

This review adapts established distinctions among vascular organization, transport, and host connection into a non-ordinal record of assay, compartment, endothelial source, observation time, model context, and construct relevance. Its conceptual contribution is the consistent application of that record to individual observations and to comparisons of printing strategies, bioinks, and wound outcomes. The vascular mechanisms, assay families, and need for product-specific validation derive from prior experimental and review literature. The proposed arrangement and reporting set remain unvalidated and require testing for clarity and reproducibility. Preserved queries and core registers support traceability, while incomplete screening records, retrieval caps, and full-text availability limit coverage.

Acknowledgments

None.

Funding

None.

Conflict of interest

The authors declare no competing interests.

Author contributions

Conceptualization: Heng Wang
Data curation: Heng Wang
Investigation: Heng Wang, Zhijian Liu
Project administration: Lei Ru
Supervision: Xuwen Li
Validation: Heng Wang, Zhijian Liu
Visualization: Heng Wang
Writing–original draft: Heng Wang
Writing–review & editing: Lei Ru, Zhijian Liu, Xuwen Li

Ethics approval and consent to participate

Not applicable.

Consent for publication

Not applicable.

Availability of data

The study extraction records and preserved literature-search information supporting this narrative review

are provided in Supplementary Tables 1–4 and the Supplementary Methods Notes.

AI tools statement

ChatGPT (OpenAI; GPT-5) and DeepSeek (V4) were used for literature and source checking, evidence organization, scientific consistency checks, and assistance with manuscript drafting and revision.

References

1. Chortova M, Zanzov E, Anastasova V. Application of 3D-Bioprinting in Treatment of Chronic Wounds: A Review. *Life (Basel)*. 2026;16(4):581.

   doi: 10.3390/life16040581

2. Masri S, Zawani M, Zulkiflee I, *et al*. Cellular Interaction of Human Skin Cells towards Natural Bioink via 3D-Bioprinting Technologies for Chronic Wound: A Comprehensive Review. *Int J Mol Sci*. 2022;23(1):476.

   doi: 10.3390/ijms23010476

3. Liu L, Spessot E, Lim KS, *et al*. Bioprinting vascularized skin analogs: a stepwise approach. *Burns Trauma*. 2025;13:tkaf018.

   doi: 10.1093/burnst/tkaf018

4. Abuhamad AY, Masri S, Fadilah NIM, Alamassi MN, Maarof M, Fauzi MB. Application of 3D-Printed Bioinks in Chronic Wound Healing: A Scoping Review. *Polymers (Basel)*. 2024;16(17):2456.

   doi: 10.3390/polym16172456

5. Derman ID, Rivera T, Garriga Cerda L, *et al*. Advancements in 3D skin bioprinting: processes, bioinks, applications and sensor integration. *Int J Extrem Manuf*. 2025;7(1):012009.

   doi: 10.1088/2631-7990/ad878c

6. Weng T, Zhang W, Xia Y, *et al*. 3D bioprinting for skin tissue engineering: Current status and perspectives. *J Tissue Eng*. 2021;12:20417314211028574.

   doi: 10.1177/20417314211028574

7. Kang MS, Jang J, Jo HJ, *et al*. Advances and Innovations of 3D Bioprinting Skin. *Biomolecules*. 2023;13(1):55.

   doi: 10.3390/biom13010055

8. Manita PG, Garcia-Orue I, Santos-Vizcaino E, Hernandez RM, Igartua M. 3D Bioprinting of Functional Skin Substitutes: From Current Achievements to Future Goals. *Pharmaceuticals (Basel)*. 2021;14(4):362.

   doi: 10.3390/ph14040362

9. Zhang M, Zhang C, Li Z, Fu X, Huang S. Advances in 3D skin bioprinting for wound healing and disease modeling. *Regen Biomater*. 2023;10:rbac105.

   doi: 10.1093/rb/rbac105

10. Gopakumar N, Ali AM, Oudda S, Singam A, Park S. 3D-Bioprinted Skin Tissues for Improving Wound Healing: Current Status and Perspective. *Adv Exp Med Biol*. 2025;1474:35-51.

    doi: 10.1007/5584_2024_817

11. Iqbal MZ, Riaz M, Biedermann T, Klar AS. Breathing new life into tissue engineering: exploring cutting-edge vascularization strategies for skin substitutes. *Angiogenesis*. 2024;27(4):587-621.

    doi: 10.1007/s10456-024-09928-6

12. Phua QH, Han HA, Soh BS. Translational stem cell therapy: vascularized skin grafts in skin repair and regeneration. *J Transl Med*. 2021;19(1):83.

    doi: 10.1186/s12967-021-02752-2

13. Smandri A, Nordin A, Hwei NM, Chin KY, Abd Aziz I, Fauzi MB. Natural 3D-Printed Bioinks for Skin Regeneration and Wound Healing: A Systematic Review. *Polymers (Basel)*. 2020;12(8):1782.

    doi: 10.3390/polym12081782

14. Fang H, Xu J, Ma H, *et al*. Functional materials of 3D bioprinting for wound dressings and skin tissue engineering applications: A review. *Int J Bioprint*. 2023;9(5):757.

    doi: 10.18063/ijb.757

15. Kızılkurtlu AA, Yılmaz Ö. A Roadmap to Perfused Skin: Defining the Next Generation of Research Questions in Cutaneous Tissue Engineering. *Int J Mol Sci*. 2026;27(12):5350.

    doi: 10.3390/ijms27125350

16. Perez-Barreto A, Moscalu R, Tremolada C, Domingos M, Reid A, Wong J. 3D bioprinting of skin equivalents: Towards functional wound healing models. *J Tissue Eng*. 2026;17:20417314251407023.

    doi: 10.1177/20417314251407023

17. Jorgensen AM, Varkey M, Gorkun A, *et al*. Bioprinted Skin Recapitulates Normal Collagen Remodeling in Full-Thickness Wounds. *Tissue Eng Part A*. 2020;26(9-10):512-526.

    doi: 10.1089/ten.tea.2019.0319

18. Luo Y, Li D, Lin C, Zhang B, Ding H, Zhou X. Construction of gelatin methacryloyl-based artificial skin substitutes with "small-micro" vascular networks via hybrid double-crosslinked coaxial and extrusion bioprinting. *Int J Bioprint*. 2026;12(1):672-688.

    doi: 10.36922/ijb025490504

19. Xia S, Weng T, Jin R, *et al*. Curcumin-incorporated 3D bioprinting gelatin methacryloyl hydrogel reduces reactive oxygen species-induced adipose-derived stem cell apoptosis

and improves implanting survival in diabetic wounds. *Burns Trauma*. 2022;10:tkac001.

doi: 10.1093/burnst/tkac001

20. Shah KR, Garriga-Cerda L, Pappalardo A, *et al*. A biopsy-sized 3D skin model with a perifollicular vascular plexus enables studying immune cell trafficking in the skin. *Biofabrication*. 2024;16(4):045006.

doi: 10.1088/1758-5090/ad5d1a

21. Maggiotto F, Dalla Valle E, Fietta A, Visentin LM, Giomo M, Cimetta E. 3D bioprinting of a perfusable skin-on-chip model suitable for drug testing and wound healing studies. *Mater Today Bio*. 2025;33:101974.

doi: 10.1016/j.mtbio.2025.101974

22. Baltazar T, Merola J, Catarino C, *et al*. Three Dimensional Bioprinting of a Vascularized and Perfusable Skin Graft Using Human Keratinocytes, Fibroblasts, Pericytes, and Endothelial Cells. *Tissue Eng Part A*. 2020;26(5-6):227-238.

doi: 10.1089/ten.tea.2019.0201

23. Baltazar T, Jiang B, Moncayo A, *et al*. 3D bioprinting of an implantable xeno-free vascularized human skin graft. *Bioeng Transl Med*. 2023;8(1):e10324.

doi: 10.1002/btm2.10324

24. Zhao M, Wang J, Zhang J, *et al*. Functionalizing multi-component bioink with platelet-rich plasma for customized in-situ bilayer bioprinting for wound healing. *Mater Today Bio*. 2022;16:100334.

doi: 10.1016/j.mtbio.2022.100334

25. Xu L, Zhang Z, Jorgensen AM, *et al*. Bioprinting a skin patch with dual-crosslinked gelatin (GelMA) and silk fibroin (SilMA): An approach to accelerating cutaneous wound healing. *Mater Today Bio*. 2023;18:100550.

doi: 10.1016/j.mtbio.2023.100550

26. Albanna M, Binder KW, Murphy SV, *et al*. In Situ Bioprinting of Autologous Skin Cells Accelerates Wound Healing of Extensive Excisional Full-Thickness Wounds. *Sci Rep*. 2019;9(1):1856.

doi: 10.1038/s41598-018-38366-w

27. Levin AA, Karalkin PA, Koudan EV, *et al*. Commercial articulated collaborative in situ 3D bioprinter for skin wound healing. *Int J Bioprint*. 2023;9(2):675.

doi: 10.18063/ijb.v9i2.675

28. Wang X, Yang C, Yu Y, Zhao Y. In Situ 3D Bioprinting Living Photosynthetic Scaffolds for Autotrophic Wound Healing. *Research (Wash D C)*. 2022;2022:9794745.

doi: 10.34133/2022/9794745

29. Dutta SD, An JM, Hexiu J, *et al*. 3D bioprinting of engineered exosomes secreted from M2-polarized macrophages through immunomodulatory biomaterial promotes in vivo wound healing and angiogenesis. *Bioact Mater*. 2025;45:345-362.

doi: 10.1016/j.bioactmat.2024.11.026

30. Kang Y, Xu L, Dong J, *et al*. Programmed microalgae-gel promotes chronic wound healing in diabetes. *Nat Commun*. 2024;15(1):1042.

doi: 10.1038/s41467-024-45101-9

31. Ferroni L, D'Amora U, Gardin C, *et al*. Stem cell-derived small extracellular vesicles embedded into methacrylated hyaluronic acid wound dressings accelerate wound repair in a pressure model of diabetic ulcer. *J Nanobiotechnology*. 2023;21(1):469.

doi: 10.1186/s12951-023-02202-9

32. Yeo M, Sarkar A, Singh YP, Derman ID, Datta P, Ozbolat IT. Synergistic coupling between 3D bioprinting and vascularization strategies. *Biofabrication*. 2024;16(1):012003.

doi: 10.1088/1758-5090/ad0b3f

33. Douglas A, Chen Y, Elloso M, Levschuk A, Jeschke MG. Bioprinting-By-Design of Hydrogel-Based Biomaterials for In Situ Skin Tissue Engineering. *Gels*. 2025;11(2):110.

doi: 10.3390/gels11020110

34. Tan CT, Liang K, Ngo ZH, Dube CT, Lim CY. Application of 3D Bioprinting Technologies to the Management and Treatment of Diabetic Foot Ulcers. *Biomedicines*. 2020;8(10):441.

doi: 10.3390/biomedicines8100441

35. Seria E, Galea G, Borg J, *et al*. Novel leukocyte-depleted platelet-rich plasma-based skin equivalent as an in vitro model of chronic wounds: a preliminary study. *BMC Mol Cell Biol*. 2021;22(1):28.

doi: 10.1186/s12860-021-00366-6

36. Botusan IR, Sunkari VG, Savu O, *et al*. Stabilization of HIF-1α is critical to improve wound healing in diabetic mice. *Proc Natl Acad Sci USA*. 2008;105(49):19426-19431.

doi: 10.1073/pnas.0805230105

37. Mirza RE, Fang MM, Ennis WJ, Koh TJ. Blocking Interleukin-1β Induces a Healing-Associated Wound Macrophage Phenotype and Improves Healing in Type 2 Diabetes. *Diabetes*. 2013;62(7):2579-2587.

doi: 10.2337/db12-1450

38. Mirza RE, Fang MM, Weinheimer-Haus EM, Ennis WJ, Koh TJ. Sustained Inflammasome Activity in Macrophages Impairs Wound Healing in Type 2 Diabetic Humans and Mice. *Diabetes*. 2014;63(3):1103-1114.

doi: 10.2337/db13-0927

39. Fu C, Liu G, Fan Y, *et al*. Highly printable and multifunctional cell-laden collagen-based bioinks for precise DLP bioprinting and rapid diabetic wound regeneration. *Mater Today Bio*. 2025;32:101908.

doi: 10.1016/j.mtbio.2025.101908

40. Huang J, Yang R, Jiao J, *et al*. A click chemistry-mediated all-peptide cell printing hydrogel platform for diabetic wound healing. *Nat Commun*. 2023;14(1):7856.

doi: 10.1038/s41467-023-43364-2

41. Zur Y, Hayam R, Almog N, *et al*. 3D Printing of Oxygen-Sensing ECM-Based Skin Graft for Personalized Treatment of Chronic Wounds-A Technological Proof of Concept. *J Funct Biomater*. 2026;17(1):28.

doi: 10.3390/jfb17010028

42. Li Z, Zheng A, Mao Z, *et al*. Silk fibroin-gelatin photo-crosslinked 3D-bioprinted hydrogel with MOF-methylene blue nanoparticles for infected wound healing. *Int J Bioprint*. 2023;9(5):773.

doi: 10.18063/ijb.773

43. Wang X, Jia J, Niu M, Li W, Zhao Y. Living Chinese Herbal Scaffolds from Microfluidic Bioprinting for Wound Healing. *Research (Wash D C)*. 2023;6:0138.

doi: 10.34133/research.0138

44. Demaria M, Ohtani N, Youssef SA, *et al*. An Essential Role for Senescent Cells in Optimal Wound Healing through Secretion of PDGF-AA. *Dev Cell*. 2014;31(6):722-733.

doi: 10.1016/j.devcel.2014.11.012

45. Pazhouhnia Z, Noori A, Farzin A, *et al*. 3D-bioprinted GelMA/gelatin/amniotic membrane extract (AME) scaffold loaded with keratinocytes, fibroblasts, and endothelial cells for skin tissue engineering. *Sci Rep*. 2024;14(1):12670.

doi: 10.1038/s41598-024-62926-y

46. Lee D, Lee S, Lee J, *et al*. Vascularized skin tissue models featuring adipose cell spheroid-laden GelMA hydrogels. *Mater Today Bio*. 2025;32:101835.

doi: 10.1016/j.mtbio.2025.101835

47. Liu Y, Liu X, Guo H, *et al*. 3D bioprinting bioglass to construct vascularized full-thickness skin substitutes for wound healing. *Mater Today Bio*. 2024;24:100899.

doi: 10.1016/j.mtbio.2023.100899

48. Tanadchangsaeng N, Pasanaphong K, Tawonsawatruk T, *et al*. 3D bioprinting of fish skin-based gelatin methacryloyl (GelMA) bio-ink for use as a potential skin substitute. *Sci Rep*. 2024;14(1):23240.

doi: 10.1038/s41598-024-73774-1

49. Wang H, Wan J, Zhang Z, Hou R. Recent advances on 3D-bioprinted gelatin methacrylate hydrogels for tissue engineering in wound healing: A review of current applications and future prospects. *Int Wound J*. 2024;21(4):e14533.

doi: 10.1111/iwj.14533

50. Wang Y, Yuan X, Yao B, Zhu S, Zhu P, Huang S. Tailoring bioinks of extrusion-based bioprinting for cutaneous wound healing. *Bioact Mater*. 2022;17:178-194.

doi: 10.1016/j.bioactmat.2022.01.024

51. Shamasha R, Ramanathan SK, Oskarsdotter K, *et al*. Biphasic Granular Bioinks for Biofabrication of High Cell Density Constructs for Dermal Regeneration. *Adv Healthc Mater*. 2025;14(21):e2501430.

doi: 10.1002/adhm.202501430

52. Kanokova D, Matejka R, Zaloudkova M, Zigmond J, Supova M, Matejkova J. Active Media Perfusion in Bioprinted Highly Concentrated Collagen Bioink Enhances the Viability of Cell Culture and Substrate Remodeling. *Gels*. 2024;10(5):316.

doi: 10.3390/gels10050316

53. Shiwarski DJ, Hudson AR, Tashman JW, *et al*. 3D bioprinting of collagen-based high-resolution internally perfusable scaffolds for engineering fully biologic tissue systems. *Sci Adv.* 2025;11(17):eadu5905.

doi: 10.1126/sciadv.adu5905

54. Jorgensen AM, Chou Z, Gillispie G, *et al*. Decellularized Skin Extracellular Matrix (dsECM) Improves the Physical and Biological Properties of Fibrinogen Hydrogel for Skin Bioprinting Applications. *Nanomaterials (Basel).* 2020;10(8):1484.

doi: 10.3390/nano10081484

55. Huang J, Lei X, Huang Z, *et al*. Bioprinted Gelatin-Recombinant Type III Collagen Hydrogel Promotes Wound Healing. *Int J Bioprint*. 2022;8(2):517.

doi: 10.18063/ijb.v8i2.517

56. Yang Y, Xu R, Wang C, Guo Y, Sun W, Ouyang L. Recombinant Human Collagen-Based Bioinks for the 3D Bioprinting of Full-thickness Human Skin Equivalent. *Int J Bioprint*. 2022;8(4):611.

doi: 10.18063/ijb.v8i4.611

57. Guan G, Lv Q, Liu S, Jiang Z, Zhou C, Liao W. 3D-bioprinted peptide coupling patches for wound healing. *Mater Today Bio*. 2022;13:100188.

doi: 10.1016/j.mtbio.2021.100188

58. Wu Y, Liang T, Hu Y, *et al*. 3D bioprinting of integral ADSCs-NO hydrogel scaffolds to promote severe burn wound healing. *Regen Biomater*. 2021;8(3):rbab014.

doi: 10.1093/rb/rbab014

59. Bashiri Z, Rajabi Fomeshi M, Ghasemi Hamidabadi H, *et al*. 3D-printed placental-derived bioinks for skin tissue regeneration with improved angiogenesis and wound healing properties. *Mater Today Bio.* 2023;20:100666.

doi: 10.1016/j.mtbio.2023.100666

60. Abaci HE, Guo Z, Coffman A, *et al*. Human Skin Constructs with Spatially Controlled Vasculature Using Primary

and iPSC-Derived Endothelial Cells. *Adv Healthc Mater*. 2016;5(14):1800-1807.

doi: 10.1002/adhm.201500936

61. Zheng Y, Chen J, Craven M, *et al*. In vitro microvessels for the study of angiogenesis and thrombosis. *Proc Natl Acad Sci USA*. 2012;109(24):9342-9347.

doi: 10.1073/pnas.1201240109

62. Wang K, Lan X, Chen J, *et al*. One-Step Coaxial 3D Printing of Pre-Vascularized Skin Organoid Models with ADSC Microspheres for Enhanced Wound Healing. *Adv Sci (Weinh)*. 2026;13(9):e17409.

doi: 10.1002/advs.202517409

63. Nessbach P, Schwarz S, Becke TD, Clausen-Schaumann H, Machens HG, Sudhop S. Angiogenic Potential of Co-Cultured Human Umbilical Vein Endothelial Cells and Adipose Stromal Cells in Customizable 3D Engineered Collagen Sheets. *J Funct Biomater*. 2022;13(3):107.

doi: 10.3390/jfb13030107

64. Kang R, Shin S, Choi Y, *et al*. Bioengineered Skin Grafts from Patient-Derived Decellularized Extracellular Matrix and Autologous Cells for Personalized Regenerative. *Adv Sci (Weinh)*. 2025;12(44):e11889.

doi: 10.1002/advs.202511889

65. Ma X, Zhu X, Lv S, *et al*. 3D bioprinting of prefabricated artificial skin with multicomponent hydrogel for skin and hair follicle regeneration. *Theranostics*. 2025;15(7):2933-2950.

doi: 10.7150/thno.104854

66. Zhang D, Fu Q, Fu H, Zeng J, Jia L, Chen M. 3D-bioprinted human lipoaspirate-derived cell-laden skin constructs for healing of full-thickness skin defects. *Int J Bioprint*. 2023;9(4):718.

doi: 10.18063/ijb.718

67. Yao R, Alkhawtani AYF, Chen R, Luan J, Xu M. Rapid and efficient in vivo angiogenesis directed by electro-assisted bioprinting of alginate/collagen microspheres with human umbilical vein endothelial cell coating layer. *Int J Bioprint*. 2019;5(2.1):194.

doi: 10.18063/ijb.v5i2.1.194

68. Schmitt T, Katz N, Kishore V. A Feasibility Study on 3D Bioprinting of Microfat Constructs Towards Wound Healing Applications. *Front Bioeng Biotechnol*. 2021;9:707098.

doi: 10.3389/fbioe.2021.707098

69. Louis F, Piantino M, Liu H, *et al*. Bioprinted Vascularized Mature Adipose Tissue with Collagen Microfibers for Soft Tissue Regeneration. *Cyborg Bionic Syst*. 2021;2021:1412542.

doi: 10.34133/2021/1412542

70. Kim J, Lee J, Cho JK, Bong KW, Song SC. Thermo-responsive Bioink for Personalized 3D Printed Scaffolds with Antioxidant and Fibroblast Delivery to Accelerate Diabetic Wound Healing. *Biomater Res*. 2025;29:0216.

doi: 10.34133/bmr.0216

71. Kim N, Lee H, Han G, *et al*. 3D-Printed Functional Hydrogel by DNA-Induced Biomineralization for Accelerated Diabetic Wound Healing. *Adv Sci (Weinh)*. 2023;10(17):e2300816.

doi: 10.1002/advs.202300816

72. Wang L, Li X, Zhang X, *et al*. Comparative regenerative mechanisms of adipose-derived mesenchymal stem cell- and conditioned medium-loaded three-dimensional bioprinted hydrogels in chronic diabetic wounds. *Regen Biomater*. 2026;13:rbag095.

doi: 10.1093/rb/rbag095

73. Zhang Y, Liao H, Wei X, *et al*. A 3-Dimensional Bioprinted Decellularized Umbilical Cord Matrix Patch for Enhanced Storage and Delivery of Extracellular Vesicles in Diabetic Wound Healing. *Research (Wash D C)*. 2026;9:1246.

doi: 10.34133/research.1246

74. Yan Z, Li R, Gao W, *et al*. pH-responsive printable conductive hydrogels loaded with ApoVs promote diabetic wound repair through oxidative stress scavenging and macrophage reprogramming. *Mater Today Bio*. 2026;37:102882.

doi: 10.1016/j.mtbio.2026.102882

75. Zhang F, Zhang Z, Duan X, *et al*. Integrating zinc/silicon dual ions with 3D-printed GelMA hydrogel promotes in situ hair follicle regeneration. *Int J Bioprint*. 2023;9(3):703.

doi: 10.18063/ijb.703

76. Fuchs B, Mert S, Hofmann D, *et al*. Bioactivated scaffolds promote angiogenesis and lymphangiogenesis for dermal regeneration in vivo. *J Tissue Eng*. 2025;16:20417314251317542.

doi: 10.1177/20417314251317542

77. Cao X, Wang Y, Xu Y, *et al*. Three-dimensional-printed ROS-scavenging and immunomodulatory hydrogel accelerates diabetic wound healing through synergistic microenvironment regulation. *Regen Biomater*. 2026;13:rbag066.

doi: 10.1093/rb/rbag066

78. Zhang C, Fang Y, Pan L, *et al*. 3D-bioprinted asymmetric bilayer scaffolds with anti-infection and pro-regeneration characteristics for chronic diabetic wound healing. *Int J Bioprint*. 2026;12(2):026120099.

doi: 10.36922/IJB026120099

79. Cao W, Li D, Yang Q, *et al*. 3D-bioprinted skin-mimicking bilayer hydrogel dressing with compartmentalized antibacterial and pro-healing functions for diabetic wounds. *Int J Bioprint*. 2026;12(3):026150134.

doi: 10.36922/IJB026150134

80. Pontiggia L, Van Hengel IA, Klar A, *et al*. Bioprinting and plastic compression of large pigmented and vascularized human dermo-epidermal skin substitutes by means of a new robotic platform. *J Tissue Eng*. 2022;13:20417314221088513.

doi: 10.1177/20417314221088513

81. Anthon SG, Valente KP. Vascularization Strategies in 3D Cell Culture Models: From Scaffold-Free Models to 3D Bioprinting. *Int J Mol Sci*. 2022;23(23):14582.

doi: 10.3390/ijms232314582

82. Chen J, Wu Y, Huang J, *et al*. Microscopically Adaptable Bioink Guide Cell Compartmentalization toward Morphogenesis of a Functional Vasculature-Like System. *Adv Healthc Mater*. 2025;14(29):e02347.

doi: 10.1002/adhm.202502347

83. Miller JS, Stevens KR, Yang MT, *et al*. Rapid casting of patterned vascular networks for perfusable engineered three-dimensional tissues. *Nat Mater*. 2012;11(9):768-774.

doi: 10.1038/nmat3357

84. Kolesky DB, Homan KA, Skylar-Scott MA, Lewis JA. Three-dimensional bioprinting of thick vascularized tissues. *Proc Natl Acad Sci USA*. 2016;113(12):3179-3184.

doi: 10.1073/pnas.1521342113

85. Kim JH, Park M, Shim JH, Yun WS, Jin S. Multi-scale vascularization strategy for 3D-bioprinted tissue using coaxial core–shell pre-set extrusion bioprinting and biochemical factors. *Int J Bioprint*. 2023;9(4):726.

doi: 10.18063/ijb.726

86. You S, Xiang Y, Hwang HH, *et al*. High cell density and high-resolution 3D bioprinting for fabricating vascularized tissues. *Sci Adv*. 2023;9(8):eade7923.

doi: 10.1126/sciadv.ade7923

87. Wang D, Maharjan S, Kuang X, *et al*. Microfluidic bioprinting of tough hydrogel-based vascular conduits for functional blood vessels. *Sci Adv*. 2022;8(43):eabq6900.

doi: 10.1126/sciadv.abq6900

88. Wang X, Liu X, Liu W, *et al*. 3D bioprinting microgels to construct implantable vascular tissue. *Cell Prolif*. 2023;56(5):e13456.

doi: 10.1111/cpr.13456

89. Szklanny AA, Machour M, Redenski I, *et al*. 3D Bioprinting of Engineered Tissue Flaps with Hierarchical Vessel Networks (VesselNet) for Direct Host-To-Implant Perfusion. *Adv Mater*. 2021;33(42):e2102661.

doi: 10.1002/adma.202102661

90. Mou S, Zhou Y, Suo L, *et al*. 3D bioprinting of flap-tissue with heterogenous cells and flexible perfusable vessels. *Bioact Mater*. 2026;65:167-180.

doi: 10.1016/j.bioactmat.2026.05.029

91. Wufuer M, Lee G, Hur W, *et al*. Skin-on-a-chip model simulating inflammation, edema and drug-based treatment. *Sci Rep*. 2016;6(1):37471.

doi: 10.1038/srep37471

92. Jones CFE, Di Cio S, Connelly JT, Gautrot JE. Design of an Integrated Microvascularized Human Skin-on-a-Chip Tissue Equivalent Model. *Front Bioeng Biotechnol*. 2022;10:915702.

doi: 10.3389/fbioe.2022.915702

93. Mazari-Arrighi E, Lépine M, Ayollo D, *et al*. Self-Organization of Long-Lasting Human Endothelial Capillary-Like Networks Guided by DLP Bioprinting. *Adv Healthc Mater*. 2024;13(14):e2302830.

doi: 10.1002/adhm.202302830

94. Figueiredo L, Le Visage C, Weiss P, Yang J. Quantifying Oxygen Levels in 3D Bioprinted Cell-Laden Thick Constructs with Perfusable Microchannel Networks. *Polymers (Basel)*. 2020;12(6):1260.

doi: 10.3390/polym12061260

95. Hudson AR, Shiwarski DJ, Kramer AJ, Feinberg AW. Enhancing Viability in Static and Perfused 3D Tissue Constructs Using Sacrificial Gelatin Microparticles. *ACS Biomater Sci Eng*. 2025;11(5):2888-2897.

doi: 10.1021/acsbiomaterials.4c02169

96. Dudaryeva OY, Buchholz MB, Größbacher G, *et al*. Multi-scale Engineered Vasculature and Hierarchical Porosity via Volumetric Bioprinting-Guided Photopolymerization-Induced Phase Separation. *Adv Mater*. 2026;38(9):e21171.

doi: 10.1002/adma.202521171

97. Vuerich R, Groppa E, Vodret S, *et al*. Ischemic wound revascularization by the stromal vascular fraction relies on host-donor hybrid vessels. *npj Regen Med*. 2023;8(1):8.

doi: 10.1038/s41536-023-00283-6

98. Fischer EO, Tsukerman A, Machour M, *et al*. Bioprinting Perfusable and Vascularized Skeletal Muscle Flaps for the Treatment of Volumetric Muscle Loss. *Adv Healthc Mater*. 2025;14(13):e2404542.

doi: 10.1002/adhm.202404542

99. Gensler M, Malkmus C, Ockermann P, *et al*. Perfusable Tissue Bioprinted into a 3D-Printed Tailored Bioreactor System. *Bioengineering (Basel)*. 2024;11(1):68.

doi: 10.3390/bioengineering11010068

100. Wu X, Zhao F, Wang H, Schirhagl R, Włodarczyk-Biegun MK. Integrating melt electrowriting (MEW) PCL scaffolds with fibroblast-laden hydrogel toward vascularized skin tissue engineering. *Mater Today Bio*. 2025;31:101593.

doi: 10.1016/j.mtbio.2025.101593

101. Zuniga K, Ghousifam N, Shaffer L, *et al*. Development of

a Static Avascular and Dynamic Vascular Human Skin Equivalent Employing Collagen/Keratin Hydrogels. *Int J Mol Sci*. 2024;25(9):4992.

doi: 10.3390/ijms25094992

102. Miyazaki H, Tsunoi Y, Akagi T, Sato S, Akashi M, Saitoh D. A novel strategy to engineer pre-vascularized 3-dimensional skin substitutes to achieve efficient, functional engraftment. *Sci Rep*. 2019;9(1):7797.

doi: 10.1038/s41598-019-44113-6

103. Zielinska D, Fisch P, Moehrlen U, *et al*. Combining bioengineered human skin with bioprinted cartilage for ear reconstruction. *Sci Adv*. 2023;9(40):eadh1890.

doi: 10.1126/sciadv.adh1890

104. Dai NT, Huang WS, Chang FW, *et al*. Development of a Novel Pre-Vascularized Three-Dimensional Skin Substitute Using Blood Plasma Gel. *Cell Transplant*. 2018;27(10):1535-1547.

doi: 10.1177/0963689718797570

105. Tobiasova Z, Sefik E, Qin L, *et al*. Endothelial MHC expression is required to initiate T cell-mediated rejection of 3D-printed skin grafts. *JCI Insight*. 2026;11(8):e201946.

doi: 10.1172/jci.insight.201946

106. Hindle SA, Bachas Brook H, Chrysanthou A, Chambers ES, Caley MP, Connelly JT. Replicating Dynamic Immune Responses at Single-Cell Resolution within a Microfluidic Human Skin Equivalent. *Adv Sci (Weinh)*. 2025;12(10):2415717.

doi: 10.1002/advs.202415717

107. Sun S, Jin L, Zheng Y, Zhu J. Modeling human HSV infection via a vascularized immune-competent skin-on-chip platform. *Nat Commun*. 2022;13(1):5481.

doi: 10.1038/s41467-022-33114-1

108. Ahmed M, Hill D, Ahmed S, Przyborski S, Dalgarno K, Dickinson A. Bioprinted autologous human skin equivalents for in vitro testing of therapeutic antibodies. *Int J Bioprint*. 2024;10(2):1851.

doi: 10.36922/ijb.1851

109. Bajuri MY, Kim J, Yu Y, Shahul Hameed MS. New Paradigm in Diabetic Foot Ulcer Grafting Techniques Using 3D-Bioprinted Autologous Minimally Manipulated Homologous Adipose Tissue (3D-AMHAT) with Fibrin Gel Acting as a Biodegradable Scaffold. *Gels*. 2023;9(1):66.

doi: 10.3390/gels9010066

110. Tojo S, Miyazaki H, Saiki T, Tsunoi Y, Nakamura S, Azuma R. Pre-Vascularized 3-Dimensional Skin Substitutes Promote Angiogenesis and Tissue Repair in a Murine Model of Refractory Skin Ulcers. *J Funct Biomater*. 2025;16(11):409.

doi: 10.3390/jfb16110409

111. Glover K, Mathew E, Pitzanti G, Magee E, Lamprou DA. 3D bioprinted scaffolds for diabetic wound-healing applications. *Drug Deliv Transl Res*. 2023;13(8):2096-2109.

doi: 10.1007/s13346-022-01115-8

112. Nuutila K, Samandari M, Endo Y, *et al*. In vivo printing of growth factor-eluting adhesive scaffolds improves wound healing. *Bioact Mater*. 2022;8:296-308.

doi: 10.1016/j.bioactmat.2021.06.030

113. Pita-Vilar M, Caicedo-Valdés D, Bravo SB, *et al*. Growth Hormone-Loaded 3D Printed Silk Fibroin-Cellulose Dressings for Ischemic Wounds. *Adv Healthc Mater*. 2026;15(5):e02969.

doi: 10.1002/adhm.202502969

114. Dong T, Hu J, Dong Y, *et al*. Advanced biomedical and electronic dual-function skin patch created through microfluidic-regulated 3D bioprinting. *Bioact Mater*. 2024;40:261-274.

doi: 10.1016/j.bioactmat.2024.06.015

115. Chen S, Xiong Y, Yang F, *et al*. Approaches to scarless burn wound healing: application of 3D printed skin substitutes with dual properties of anti-infection and balancing wound hydration levels. *eBioMedicine*. 2024;106:105258.

doi: 10.1016/j.ebiom.2024.105258

116. Yang R, Sun J, Peng G, *et al*. Synergistic promotion of diabetic wound healing by glucose-responsive functional chitosan-based composite nanohydrogels. *Carbohydr Polym*. 2026;377:124835.

doi: 10.1016/j.carbpol.2025.124835

117. Yang Z, Li R, Wang R, Qian S. Enhancing Healing of Infected Wounds with Glycerin-Modified Sodium Alginate/Silk Sericin Composite Film Functionalized with Polygonatum sibiricum Polysaccharide-Capped Silver Nanoparticles. *ChemistrySelect*. 2024;9(14):e202400566.

doi: 10.1002/slct.202400566

118. Sun Z, Liu Q, Wang Z, *et al*. Hierarchical chitosan/polyvinyl alcohol/polyethylene glycol/nonwoven fabric micro/nanofiber composite membrane: a potential biomaterial for wound dressing. *Macromol Res*. 2023;31(12):1209-1215.

doi: 10.1007/s13233-023-00204-y

119. Rocha F, Vala IS, de Oliveira P, *et al*. Low-dose ionizing radiation in vivo unlocks the therapeutic potential of prevascularized dermal spheroids in chronic wounds. *Mater Today Bio*. 2025;35:102561.

doi: 10.1016/j.mtbio.2025.102561

120. Revokatova DP, Khristidis YI, Fayzullin AL, *et al*. Portable Bioprinter in Ischemic Wound Therapy: a Pilot Study. *Sovrem Tekhnologii Med*. 2026;18(1):23-31.

doi: 10.17691/stm2026.18.1.02

121. Abellan Lopez M, Hutter L, Pagin E, *et al*. In vivo efficacy proof of concept of a large-size bioprinted dermo-epidermal substitute for permanent wound coverage. *Front Bioeng Biotechnol*. 2023;11:1217655.

doi: 10.3389/fbioe.2023.1217655

122. Kang Y, Yeo M, Derman ID, *et al*. Intraoperative bioprinting of human adipose-derived stem cells and extra-cellular matrix induces hair follicle-like downgrowths and adipose tissue formation during full-thickness craniomaxillofacial skin reconstruction. *Bioact Mater*. 2024;33:114-128.

doi: 10.1016/j.bioactmat.2023.10.034

123. Matsumura R, Matsumura H, Kawai Y, *et al*. Three-Dimensional Bioprinted Autologous Minimally Manipulated Homologous Adipose Tissue for Skin Defects After Wide Excision of Skin Cancer Provides Early Wound Closure and Good Esthetic Patient Satisfaction. *J Clin Med*. 2025;14(6):1795.

doi: 10.3390/jcm14061795

124. Yoon HM, Song WJ. Using 3D Bioprinted Autologous Minimally Manipulated Homologous Adipose Tissue for Limb Salvage in Treating Diabetic Foot Ulcer. *Arch Plast Surg*. 2024;51(3):332-336.

doi: 10.1055/a-2263-7957

125. Zhao W, Chen H, Zhang Y, *et al*. Adaptive multi-degree-of-freedom in situ bioprinting robot for hair-follicle-inclusive skin repair: A preliminary study conducted in mice. *Bioeng Transl Med*. 2022;7(3):e10303.

doi: 10.1002/btm2.10303

126. Wang C, Hu C, Cheng H, *et al*. A Programmable Handheld Extrusion-Based Bioprinting Platform for In Situ Skin Wounds Dressing: Balance Mobility and Customizability. *Adv Sci (Weinh)*. 2024;11(46):e2405823.

doi: 10.1002/advs.202405823

127. Chai RJ, Wong WL, Beh CW. Developing a bioink for single-step deposition and maturation of human epidermis. *Int J Bioprint*. 2023;9(4):738.

doi: 10.18063/ijb.738

128. Riabinin A, Pankratova M, Rogovaya O, Vorotelyak E, Terskikh V, Vasiliev A. Ideal Living Skin Equivalents, From Old Technologies and Models to Advanced Ones: The Prospects for an Integrated Approach. *Biomed Res Int*. 2024;2024(1):9947692.

doi: 10.1155/2024/9947692

129. Oualla-Bachiri W, Fernández-González A, Quiñones-Vico MI, Arias-Santiago S. From Grafts to Human Bioengineered Vascularized Skin Substitutes. *Int J Mol Sci*. 2020;21(21):8197.

doi: 10.3390/ijms21218197

130. Kondej K, Zawrzykraj M, Czerwiec K, Deptuła M, Tymińska A, Pikuła M. Bioengineering Skin Substitutes for Wound Management—Perspectives and Challenges. *Int J Mol Sci*. 2024;25(7):3702.

doi: 10.3390/ijms25073702

131. Sörgel CA, Cai A, Schmid R, Horch RE. Perspectives on the Current State of Bioprinted Skin Substitutes for Wound Healing. *Biomedicines*. 2023;11(10):2678.

doi: 10.3390/biomedicines11102678

132. Zhang T, Sheng S, Cai W, *et al*. 3-D bioprinted human-derived skin organoids accelerate full-thickness skin defects repair. *Bioact Mater*. 2024;42:257-269.

doi: 10.1016/j.bioactmat.2024.08.036

133. Fu H, Zhang D, Zeng J, *et al*. Application of 3D-printed tissue-engineered skin substitute using innovative biomaterial loaded with human adipose-derived stem cells in wound healing. *Int J Bioprint*. 2023;9(2):674.

doi: 10.18063/ijb.v9i2.674

134. Niu C, Wang L, Ji D, *et al*. Fabrication of SA/Gel/C scaffold with 3D bioprinting to generate micro-nano porosity structure for skin wound healing: a detailed animal in vivo study. *Cell Regen*. 2022;11(1):10.

doi: 10.1186/s13619-022-00113-y

135. Albouy M, Desanlis A, Brosset S, *et al*. A Preliminary Study for an Intraoperative 3D Bioprinting Treatment of Severe Burn Injuries. *Plast Reconstr Surg Glob Open*. 2022;10(1):e4056.

doi: 10.1097/gox.0000000000004056